The Journal of Neuroscience, October 1, 1999, *19*(19):8182–8198

Cellular and Molecular Mechanisms of Glial Scarring and Progressive Cavitation: *In Vivo* and *In Vitro* Analysis of Inflammation-Induced Secondary Injury after CNS Trauma

Michael T. Fitch,[1] Catherine Doller,[1] Colin K. Combs,[2] Gary E. Landreth,[2] and Jerry Silver[1]

[1]Department of Neurosciences and [2]Alzheimer Research Laboratory, Case Western Reserve University School of Medicine, Cleveland, Ohio 44106

Post-traumatic cystic cavitation, in which the size and severity of a CNS injury progress from a small area of direct trauma to a greatly enlarged secondary injury surrounded by glial scar tissue, is a poorly understood complication of damage to the brain and spinal cord. Using minimally invasive techniques to avoid primary physical injury, this study demonstrates *in vivo* that inflammatory processes alone initiate a cascade of secondary tissue damage, progressive cavitation, and glial scarring in the CNS. An *in vitro* model allowed us to test the hypothesis that specific molecules that stimulate macrophage inflammatory activation are an important step in initiating secondary neuropathology. Time-lapse video analyses of inflammation-induced cavitation in our *in vitro* model revealed that this process occurs primarily via a previously undescribed cellular mechanism involving dramatic astrocyte morphological changes and rapid migration. The physical process of cavitation leads to astrocyte abandonment of neuronal processes, neurite stretching, and secondary injury. The macrophage mannose receptor and the complement receptor type 3 β2-integrin are implicated in the cascade that induces cavity and scar formation. We also demonstrate that anti-inflammatory agents modulating transcription via the nuclear hormone receptor peroxisome proliferator–activated receptor-γ may be therapeutic in preventing progressive cavitation by limiting inflammation and subsequent secondary damage after CNS injury.

Key words: chondroitin sulfate proteoglycan; inflammation; gliosis; microglia; macrophage; astrocyte; injury; trauma; regeneration; necrosis; cavitation; mannose receptor; CR3; β-integrin; CD11b/CD18; Mac-1

Injury to the adult mammalian CNS leads to a complex series of cellular and molecular events, as cells respond to trauma and attempt to repair damaged regions of the brain or spinal cord (for review, see Fitch and Silver, 1999a). Unlike the successful healing responses in the peripheral nervous system, adult CNS injury leads to permanent disability, because most severed axons fail to regenerate (Ramon y Cajal, 1928; Guth, 1975; Reier et al., 1983). A phenomenon that adds to the complexity of regenerative failure is the process of progressive cavitation in which, after days to weeks, a CNS injury can expand in size leading to a scar-encapsulated cavity many times the size of the initial wound (Balentine, 1978). Although various hypotheses suggest that this secondary process of cavitation is related to ischemia (Balentine, 1978), hemorrhage (Ducker et al., 1971; Wallace et al., 1987), lysozyme activity (Kao et al., 1977), pulsatile hydrodynamics (Williams et al., 1981), or macrophage infiltration and inflammation (Blight, 1991a, 1994; Szczepanik et al., 1996; Fitch and Silver, 1997a; Zhang et al., 1997), the underlying causes of progressive axon damage and the cellular mechanisms that lead to cyst formation are poorly understood. Insights into this process will provide direction for therapeutic intervention designed to minimize secondary damage and lead to enhanced function after a debilitating injury.

In this study we have used both *in vivo* and *in vitro* models to test our hypothesis that post-traumatic inflammation can lead to the development of cavities in the CNS. Our results indicate that inflammatory processes induced by the *in vivo* microinjection of a single, small bolus of zymosan particles in the absence of significant physical damage are detrimental to CNS tissue and directly lead to secondary damage, progressive cavitation, and upregulation of glial scar–associated inhibitory molecules. Using a tissue culture model, we further demonstrate that the mechanism of cavitation is mediated primarily via robust astrocyte migration and morphological changes stimulated by activated macrophages that can lead to astrocyte abandonment of neuronal processes and may also lead to axonal injury. To address the issue of signaling mechanisms and triggers for these effects, we used several molecules that specifically activate macrophage cell surface receptors leading to macrophage activation and subsequent astrocyte reactions in our *in vitro* model of cavity formation. Additional results from our *in vitro* assay suggest that preventing this specific inflammatory activation with peroxisome proliferator–activated receptor (PPAR)-γ agonists, a class of anti-inflammatory agents, may provide a novel therapy for preventing progressive cavitation by limiting inflammation and its subsequent secondary damage after a CNS injury.

MATERIALS AND METHODS

Cell culture methods. Purified astrocyte cultures were generated from newborn [postnatal day 0 (P0)] Sprague Dawley rat cortices using a procedure modified from that of McCarthy and De Vellis (1980). Cere-

Received April 15, 1999; revised July 8, 1999; accepted July 12, 1999.

This work was supported by the National Institute of Neurological Disorders and Stroke Grant NS25713, the Daniel Heumann Fund, and the Brumagin Memorial Fund.

Correspondence should be addressed to Dr. Michael T. Fitch, Department of Neurosciences, Case Western Reserve University, 10900 Euclid Avenue, Cleveland, OH 44106.

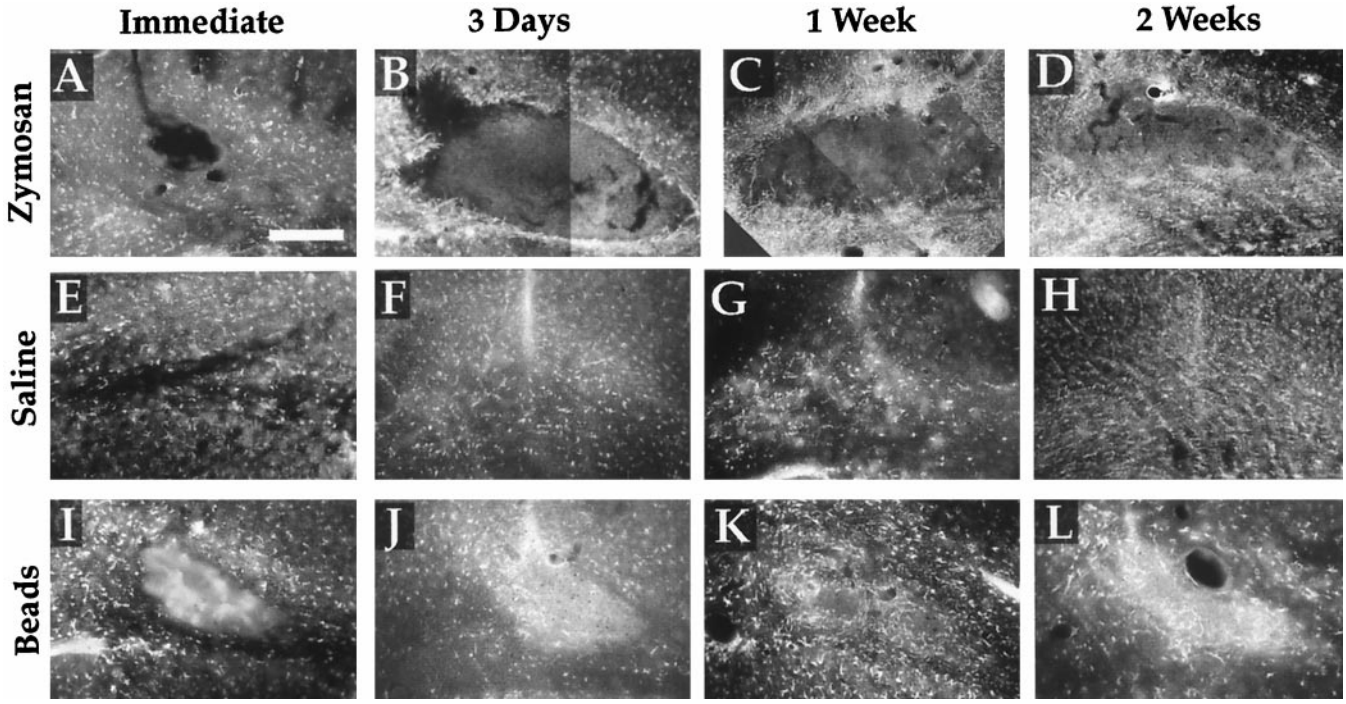

Figure 1. Astrocyte GFAP staining of statistically representative tissue sections (selected based on average cavity sizes; see Fig. 2) at the site of minimally invasive microinjections of zymosan (*A–D*; $n = 32$), saline (*E–H*; $n = 14$), or latex beads (*I–L*; $n = 10$) immediately (*A, E, I*), 3 d (*B, F, J*), 1 week (*C, G, K*), and 2 weeks (*D, H, L*) after injection. Note the enlarged astrocyte-free cavity present at 3 d (*B*) and 1 week (*C*) after microinjection of zymosan, a potent inflammatory stimulant. There is no significant increase in cavity size after saline injection (*E–H*), and no significant increase in cavity size is seen after injection of particulate latex beads (*I–K*) the same size and concentration as zymosan particles. Scale bar, 340 μm.

bral cortices were isolated, separated from meninges, and dissociated in calcium- and magnesium-free Hanks' balanced salt solution with 0.1% trypsin and 0.020% EDTA for 30 min at 37°C, with the addition of 100 μl of 2 mg/ml DNase after 15 min. DMEM-F12 medium (Life Technologies, Gaithersburg, MD) with 10% fetal calf serum (FCS; Sigma, St. Louis, MO) was added, and the tissue was triturated through a fire-polished glass pipette. Cells were grown in poly-L-lysine–coated tissue culture flasks (0.1 mg/ml) overnight at 37°C. Cultures were purified for astrocytes by vigorously shaking the flasks to remove nonadherent cells. Astrocytes were matured in culture in DMEM-F12 (10% FCS) for 10 d and used for experiments before they reached >4 weeks of age in culture.

Adult dorsal root ganglion neurons were isolated according to a previous protocol (Davies et al., 1997). Single-cell suspensions of dorsal root ganglia (DRGs) were prepared from adult (250–300 gm) Sprague Dawley rats. Lumbar and cervical DRGs were dissected, roots and capsules were removed, and suspensions were incubated in dispase (2.5 units/ml) and collagenase II (200 units/ml) for 30–60 min at 37°C, until cells would easily separate. Resuspension in DMEM-F12 and gentle trituration through a fire-polished pipette resulted in a single-cell suspension of adult DRG neurons.

Microglial cells were obtained using a modification of the procedure by Giulian and Baker (1986). Mixed glial cultures were prepared from P0 rat pups using the dissection and dissociation protocols described above. These mixed glial cultures were not shaken to remove nonadherent cells and were instead grown for 3–7 d in DMEM-F12 media supplemented with 20% fetal calf serum to enrich for microglial cells. Flasks were lightly shaken to release microglial cells into the media supernatant, and these floating microglia were subsequently spun down, washed with DMEM-F12 media, and plated in culture.

Peritoneal macrophages were obtained using modifications of the methods used by Michalek et al. (1998) and Xia et al. (1999). Three milliliters of Brewer's thioglycollate broth (Difco, Detroit, MI) were injected into the peritoneal cavity of adult Sprague Dawley rats (300 gm). After 3 d, rats were deeply anesthetized, and 50 ml of cold sterile L15 media was injected into the peritoneum and withdrawn to extract resident peritoneal macrophages. To purify the macrophage population, we collected the cells by centrifugation, resuspended them briefly in 3 ml of distilled water to lyse red blood cells, and rapidly resuspended them in 15 ml of DMEM-F12 for subsequent use in culture experiments. Conditioned media from cultured peritoneal macrophages were prepared using $5–12 \times 10^6$ macrophages per tissue culture flask, ±0.1 mg/ml zymosan in 10 ml of culture media. After 3 d, the media were removed, clarified by centrifugation, and stored at −20°C until use.

Immunocytochemistry. Tissue sections or cells grown on glass coverslips were washed in PBS, blocked with 4% normal goat serum with 0.1% Triton X-100 (Sigma), and incubated overnight in primary antibody diluted in blocking solution followed by appropriate secondary and tertiary steps in blocking solution for single-, double-, and triple-staining procedures by standard fluorescent immunocytochemical methods. Monoclonal antibodies used included CS56 (1:100; Sigma) to identify chondroitin sulfate proteoglycans, ED1 (1:250; Chemicon, Temecula, CA) for activated macrophages and microglia, RT-97 (1:100; Boehringer Mannheim, Indianapolis, IN) for neurofilament-containing axons and neurons, anti-type III β-tubulin antibody (1:100; Sigma) to label adult DRG neurons and processes in culture, and RECA-1 (1:25; Serotec, Raleigh, NC) for blood vessel endothelial cells. Polyclonal anti-GFAP antibodies were used to identify astrocyte intermediate filaments (1:300; Accurate Chemicals, Westbury, NY). Control sections that did not receive primary antibodies were used to distinguish specific staining from nonspecific antibody binding and/or autofluorescent components of lesion areas. Sections were examined using a Zeiss laser-scanning confocal microscope and/or a Leitz Orthoplan-2 fluorescence light microscope (Wetzlar, Germany).

In vivo *cavitation experiments.* Surgical procedures and microinjection techniques were performed as described previously (Anthony et al., 1997; Davies et al., 1997; Fitch and Silver, 1997a). Adult Sprague Dawley female rats (300–325 gm) were anesthetized by intramuscular ketamine (100 mg/kg) and xylazine (2.4 mg/kg). A midline scalp incision was used to access the skull, and a stereotaxic drill was used to remove a small area of bone. Stereotaxic microinjection into the brain was conducted with a glass micropipette with an outer diameter of 120 μm with a sharp beveled edge. Stereotaxic coordinates of the injections were relative to the bregma at 1 mm rostral, 2 mm lateral, and a depth of 2.5 mm. Minute quantities (0.25 and 0.5 μl) were gently injected into the white matter of the corpus callosum using a Picospritzer (General Valve, Fairfield, NJ) to cause minimal physical damage to the brain parenchyma. Zymosan

(12.5 mg/ml; Sigma; an inert particulate macrophage activator), lipopolysaccharide (LPS; 20 μg/ml; Sigma; a soluble immunostimulant), 3 μm latex microspheres (Polysciences, Warrington, PA; a particulate control used at the same particle concentration as zymosan), and PBS (a control for the injection procedure) were among the test substances used. After postoperative periods of 10–30 min, 3 d, 1 week, and 2 weeks, animals were deeply anesthetized and perfused through the aorta with 100 ml of PBS followed by 400 ml of 4% paraformaldehyde in phosphate buffer. Coronal tissue sections 60 μm thick were cut using a Vibratome and processed for immunohistochemical analysis. For quantitation of astrocyte cavity size, a single representative fluorescent photograph stained to visualize the GFAP of astrocytes was taken at the site of each initial injection needle tract. These were scanned into an Apple Macintosh computer and randomized, and the size of the cavity was measured in a blinded manner using the NIH Image analysis program. Data were subsequently analyzed using Statview statistical software with ANOVA and Fisher's PLSD for multiple comparisons.

In vitro *neuron toxicity experiments.* Adult DRGs were plated at a density of 5000–6000 neurons per well in 24-well tissue culture plates on glass coverslips coated with poly-L-lysine (0.1 mg/ml) and laminin (5 μg/ml). In some experiments, DRG neurons were grown on astrocyte monolayers to model more closely the normal cellular associations found *in vivo*. After 24 hr of growth in culture, microglial cells or peritoneal macrophages were added to each of the wells at a density of 50,000 cells per well. Nonactivated macrophages or microglial cells served as controls and were compared with zymosan-activated (0.1 mg/ml) macrophages or microglial cells. After 24 hr or 3 d of coculture of macrophages and DRGs, propidium iodide (50 μg/ml) was used to assess cell viability by membrane integrity (Freshney, 1987) before culture fixation with 4% paraformaldehyde. The fixed cultures were stained with antibodies to β-tubulin to identify DRG neurons and their processes and with ED1 to stain macrophages and/or microglia. Separate control experiments demonstrated that zymosan treatment alone was nontoxic to DRGs alone, astrocytes alone, macrophages alone, or DRGs cultured with astrocytes.

All statistical comparisons were made between control DRG cultures with nonactivated macrophages versus DRG cultures with zymosan-activated macrophages. Each experiment was coded, randomized, and scored in a blinded manner. For each coverslip, 10 microscopic fields of view were counted from a standard grid using a low-power 16× objective. The quantitative data from each measurement group were expressed per field of view relative to the appropriate control group average being standardized to a value of 1. Data were analyzed with StatView statistical software using the nonparametric Mann–Whitney *U* test. For time-lapse video microscopy, cultures were maintained at 37°C, and still-frame–digitized images were captured by computer every minute for the course of the analysis using the Metamorph imaging software (Universal Imaging Corporation, West Chester, PA).

In vitro *cavitation assay.* Astrocytes that had been grown for at least 10 d in culture were seeded at identical densities in 24-well tissue culture plates (plating densities of 50,000–100,000 cells per well, depending on the experiment) on glass coverslips coated with poly-L-lysine (0.1 mg/ml) or poly-L-lysine and laminin (5 μg/ml) and allowed to reach confluency (1–3 d) in DMEM-F12 media with 10% heat-inactivated and sterile-filtered fetal calf serum. Peritoneal macrophages were isolated from adult Sprague Dawley rats and introduced into the astrocyte cultures at a density of 25,000–100,000 cells per well, depending on the experiment. Nonactivated macrophages (controls) were seeded in culture media only, whereas activated macrophages were introduced with 0.05 or 0.1 mg/ml Zymosan (Sigma), a potent macrophage activator. The cocultures were maintained for periods of 24 hr or 3 d. After the culture period, propidium iodide (50 μg/ml; Molecular Probes, Eugene, OR) was used to assess cell viability by membrane integrity (Freshney, 1987) before fixation of the cultures with 4% paraformaldehyde. The fixed cultures were stained with antibodies to GFAP to identify astrocytes, ED1 to stain macrophages, and 4,6-diamidino-2-phenylindole (DAPI) to label all cell nuclei. Each experimental condition was replicated at least six times in at least two independent setups, and replicates were expressed relative to their own simultaneous controls set to a value of 1 and combined for statistical analysis and presentation. Separate control cultures demonstrated that zymosan alone with astrocytes was nontoxic and did not significantly affect viability or the formation of culture cavities.

All statistical comparisons were made between control astrocyte cultures with nonactivated macrophages versus astrocyte cultures with zymosan-activated macrophages. For each experiment, six microscopic fields of view from a single coverslip were photographed from a standard grid using a low-power 16× objective. For each field of view, the numbers of dead astrocytes and macrophages stained with propidium iodide were recorded; macrophages were photographed in one fluorescent channel, and GFAP+ astrocytes and the total number of cell nuclei were photographed in another. These photographs were scanned into an Apple Macintosh computer, randomized, and analyzed blindly using NIH Image to count and subsequently calculate the numbers of astrocytes and macrophages, the cell density, and the size of culture cavities (areas of the culture devoid of astrocyte monolayers). The quantitative data from each measurement group were expressed per field of view relative to the appropriate control group average being standardized to a value of 1. Data were then analyzed with StatView statistical software using the nonparametric Mann–Whitney *U* test and ANOVA with Fisher's PLSD for multiple comparisons. Additional *post hoc* analyses were conducted on the data from Figures 9 and 13 with Scheffe's *F* test and the Bonferroni–Dunn test and yielded equivalent significance levels. For time-lapse video microscopy, cultures were maintained at 37°C, and still-frame–digitized images were captured by computer every minute for the course of the analysis using the Metamorph imaging software (Universal Imaging Corporation).

For experiments using conditioned media from activated and nonactivated macrophage cultures, the same astrocyte culture methods were used without the addition of live macrophages or zymosan-stimulant particles. The conditioned media were used full strength (100%) or diluted 1:1 with fresh media (50%) for 24 hr or 3 d of incubation. For some experiments, full-strength media (both activated and nonactivated) were heated to 60°C for 15 min before use. In other experiments, the conditioned media (both activated and nonactivated) were boiled for 40 min before 1:1 dilution with fresh media and subsequent use. Statistical comparisons were made between cultures using conditioned media from

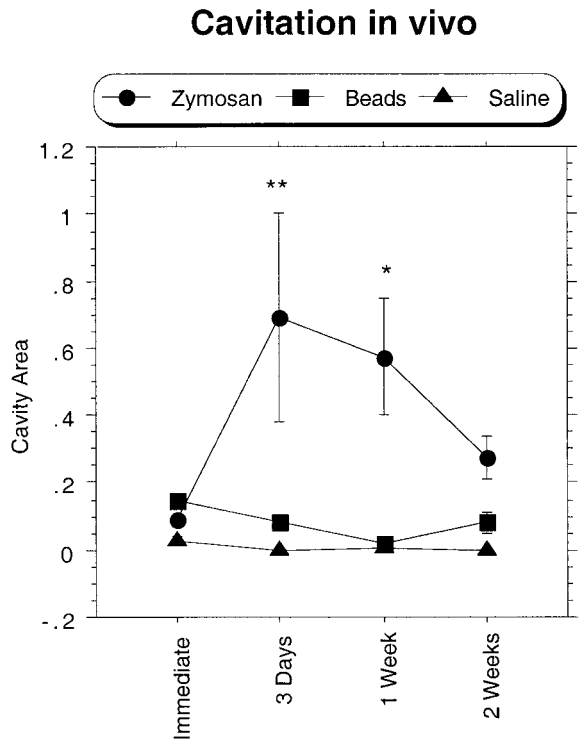

Figure 2. Graphical comparisons and statistical analysis of the average size (± SEM) of the astrocyte-free cavity areas (in mm^2) after *in vivo* callosal microinjections of zymosan ($n = 32$), saline ($n = 14$), or latex beads ($n = 10$). Cavity sizes are significantly larger than that of the immediate time point after zymosan injection at 3 d ($p < 0.01$) and 1 week ($p < 0.05$), and by 2 weeks the healing process has diminished the cavity to within control levels as astrocytes have repopulated the cavity. Injections of saline or latex beads do not lead to significant increases in cavity size at any time point. ANOVA with Fisher's PLSD is reported relative to the immediate time point for each category ($^*p < 0.05$; $^{**}p < 0.01$).

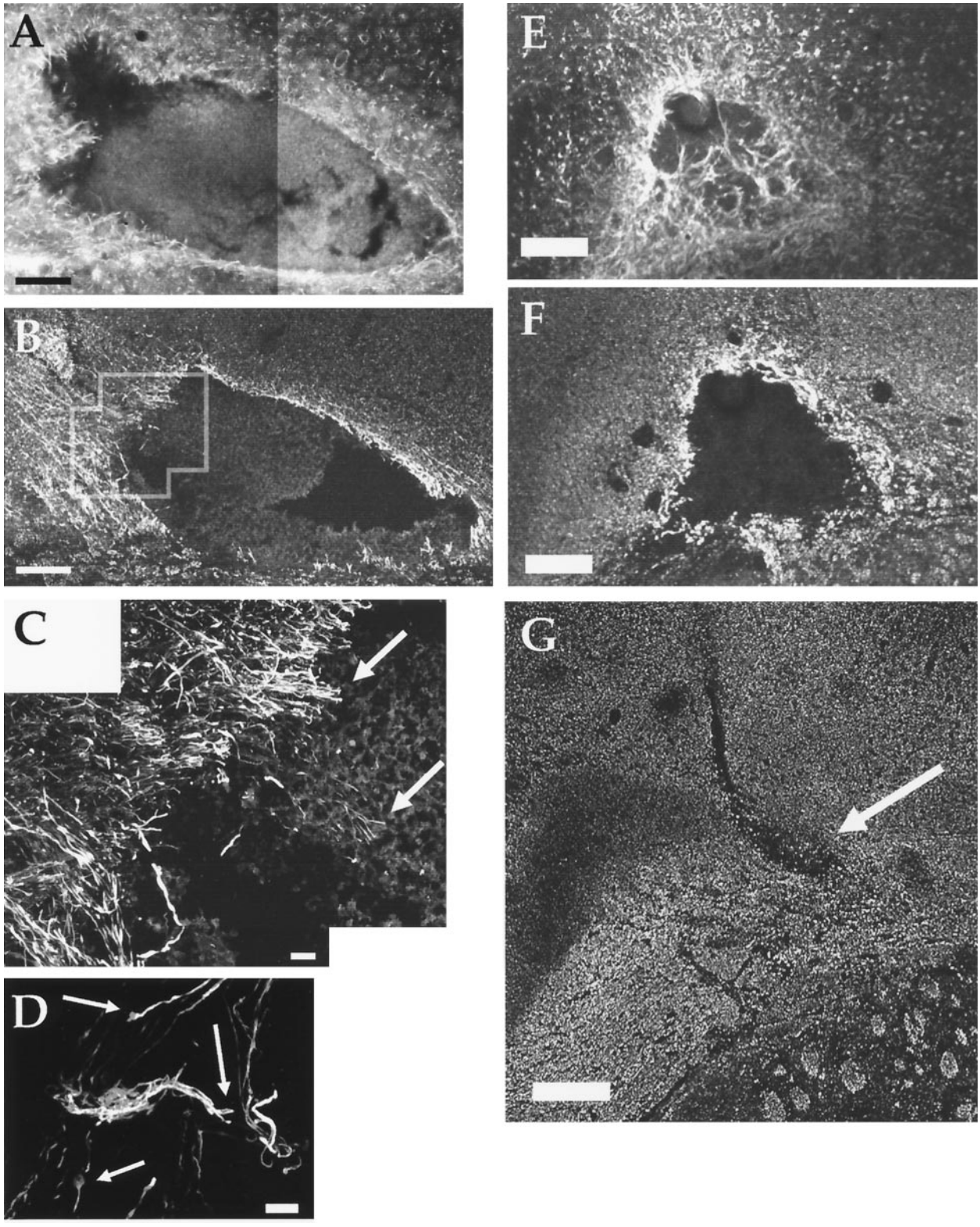

Figure 3. The area of axon damage precisely surrounds the area of astrocyte cavitation at 3 d after zymosan injection *in vivo* but does not show evidence of repair or regeneration of neurofilament-containing axons after astrocytes repopulate the cavity after 2 weeks. *A,* Astrocyte GFAP staining demarcates this white matter cavity at 3 d (same section shown in Fig. 1*B*). *B–D,* Neurofilament staining in *B* demonstrates an increased intensity in the axons at the borders of the developing cavity in an adjacent section to *A*, and ends of axons that have been secondarily damaged can be seen at high power in *C* from the *area outlined* in *B*. Dystrophic axon endings are found within the cavity (*C*; *arrows*) and are also demonstrated in another 3 d developing cavity (*D; arrows*). *E, F,* Astrocyte GFAP staining in *E* illustrates the partial filling in of the cavity by astrocytes at 2 weeks after injection, which is not mirrored by any changes in the neurofilament-containing axons as seen in *F*. *G*, These destructive effects on axons were not seen at the injection site with neurofilament staining immediately after zymosan injection (*arrow*), illustrating the minimal direct injury from the injection itself. Scale bars: *A, B*, 200 μm; *C, D*, 20 μm; *E–G,* 180 μm.

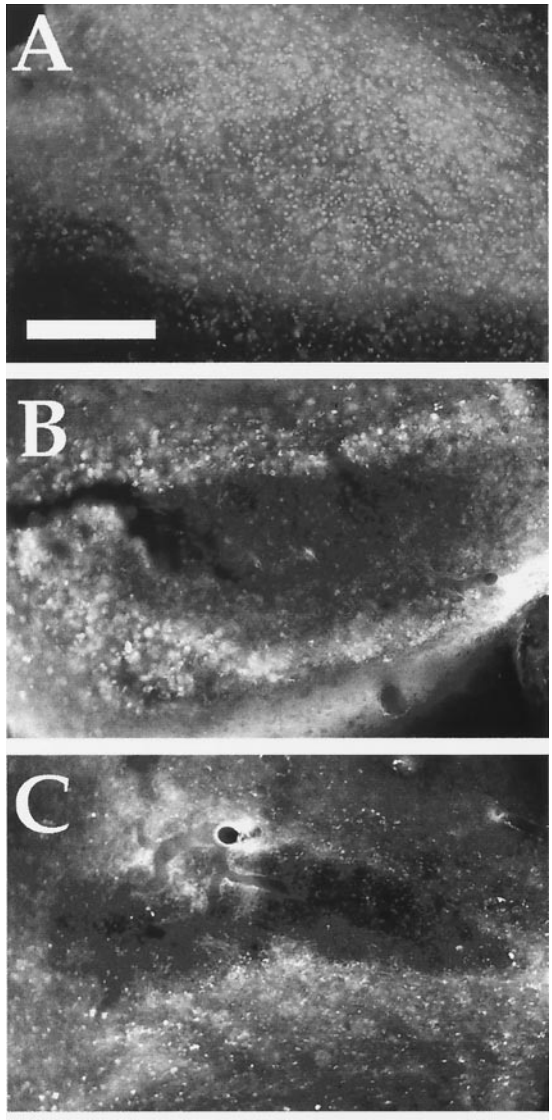

Figure 4. Fluorescent photomicrographs of zymosan-induced inflammation *in vivo* within the developing cavities 3 d (*A*), 1 week (*B*), and 2 weeks (*C*) after zymosan injection. The high concentration of activated macrophages and microglia stained with ED1 present at 3 d (*A*) gradually diminishes from 1 week (*B*) to 2 weeks (*C*). Scale bar, 340 μm.

nonactivated macrophages and conditioned media from zymosan-activated macrophages treated in identical ways.

For receptor agonist experiments, particulate β-glucan isolated from *Saccharomyces cerevisiae* (0.05 mg/ml; Sigma) and/or mannosylated bovine serum albumin (mBSA; 1 μM; E-Y Labs, San Mateo, CA) were added to macrophage cultures in the place of zymosan to stimulate specific interactions with the β-glucan–binding site of the complement receptor type 3 (CR3) integrin receptor and/or the macrophage mannose receptor, respectively (Wileman et al., 1986; Thornton et al., 1996; Engering et al., 1997; Gelderman et al., 1998; Xia et al., 1999).

For experiments examining the effects of anti-inflammatory agents, all astrocyte cultures were grown on poly-L-lysine coverslips coated with laminin, and the cocultures were maintained for 3 d with 100,000 macrophages, astrocyte monolayers, and a drug treatment. Each group had two components (nonactivated macrophages with treatment and zymosan-activated macrophages with treatment) for standardization within each group to control for any variances in drug effects on nonactivated culture preparations. The treatment groups included no treatment [vehicle only (DMSO at 1 μl/ml)], indomethacin treatment (100 μM; Sigma), prostaglandin J2 treatment (10 μM; Calbiochem, La Jolla, CA), and ciglitazone treatment (50 μM; Biomol, Plymouth Meeting, PA) of the zymosan-activated macrophages.

RESULTS

Persistent inflammation *in vivo* leads to progressive cavitation

The *in vivo* model of progressive cavitation used in this study was designed to separate persistent secondary inflammatory events that are commonly found in the vicinity of CNS injuries from those pathological changes that are a result of direct tissue damage. Using a technique that minimizes direct cellular injury (Davies et al., 1996), we were able to introduce various compounds carefully into the adult rat corpus callosum via a single microinjection of <0.5 μl. Zymosan, a nontoxic particulate yeast wall preparation used widely as a macrophage and/or microglia activator in tissue culture studies (Giulian et al., 1994; Klegeris and McGeer, 1994), was the only specific molecule we tested in this manner that was sufficiently potent *in vivo* to induce persistent inflammation leading to cavity formation and glial scarring. Other molecules tested in our *in vivo* model that were unable to initiate the cascade of cellular events leading to cavitation with only a single microinjection included interleukin-1β, transforming growth factor-β, epidermal growth factor, vascular endothelial growth factor, ciliary neurotrophic factor, thrombin, and LPS. Therefore, we used zymosan microinjections into the corpus callosum of the adult rat brain to study the effects of intense inflammation in the absence of significant direct tissue damage.

A series of control experiments conducted *in vitro* confirmed that zymosan particles were not directly toxic to cells. Zymosan particles were added separately to astrocyte cultures, adult DRG neuron cultures, cocultures of adult DRG neurons with astrocytes, and macrophage cultures. The addition of zymosan did not significantly affect numbers of live cells counted in these cultures after 24 hr or 3 d when compared with matched cultures without zymosan. Only when zymosan-activated macrophages or microglial cells were cocultured with other cells were the detrimental effects observed, consistent with results demonstrated by other investigators in which zymosan without microglia had no effect on astrocytes or neurons (Giulian et al., 1993a, 1994). The concentration of zymosan used in culture contained $\sim 25 \times 10^6$ particles in 1 ml of media, which settled down densely on top of the cells at a concentration of 1.25×10^6 particles per square millimeter of culture area.

Microinjection of 0.25 or 0.5 μl of highly concentrated sterile zymosan ($\sim 1.25 \times 10^6$ particles/0.5 μl) with a micropipette into the corpus callosum of adult Sprague Dawley rats initially produced only a very small cavity evident with astrocyte GFAP immunostaining as a direct result of the relatively atraumatic injection of the tiny bolus of particles ($n = 13$; Fig. 1*A*). By 3 d ($n = 7$; Fig. 1*B*), the persistent inflammation generated by the zymosan particles had caused a statistically significant ($p = 0.0055$; Fig. 2) sevenfold increase in the average size of the astrocyte-free cavity, a result that was maintained ($p = 0.0297$; Fig. 2) at 1 week after injection ($n = 6$; Fig. 1*C*). By 2 weeks after zymosan injection ($n = 6$; Fig. 1*D*), the cavity was beginning to resolve. As the inflammatory infiltrates diminished, astrocytes were found to be repopulating the cavity area, and the size of the cavity diminished toward the size of the initial immediate injection cavity. Figure 1 illustrates statistically representative sections (i.e., representative of the mean cavity size of each group) based on the quantitative analysis of cavity sizes at each time point seen in Figure 2.

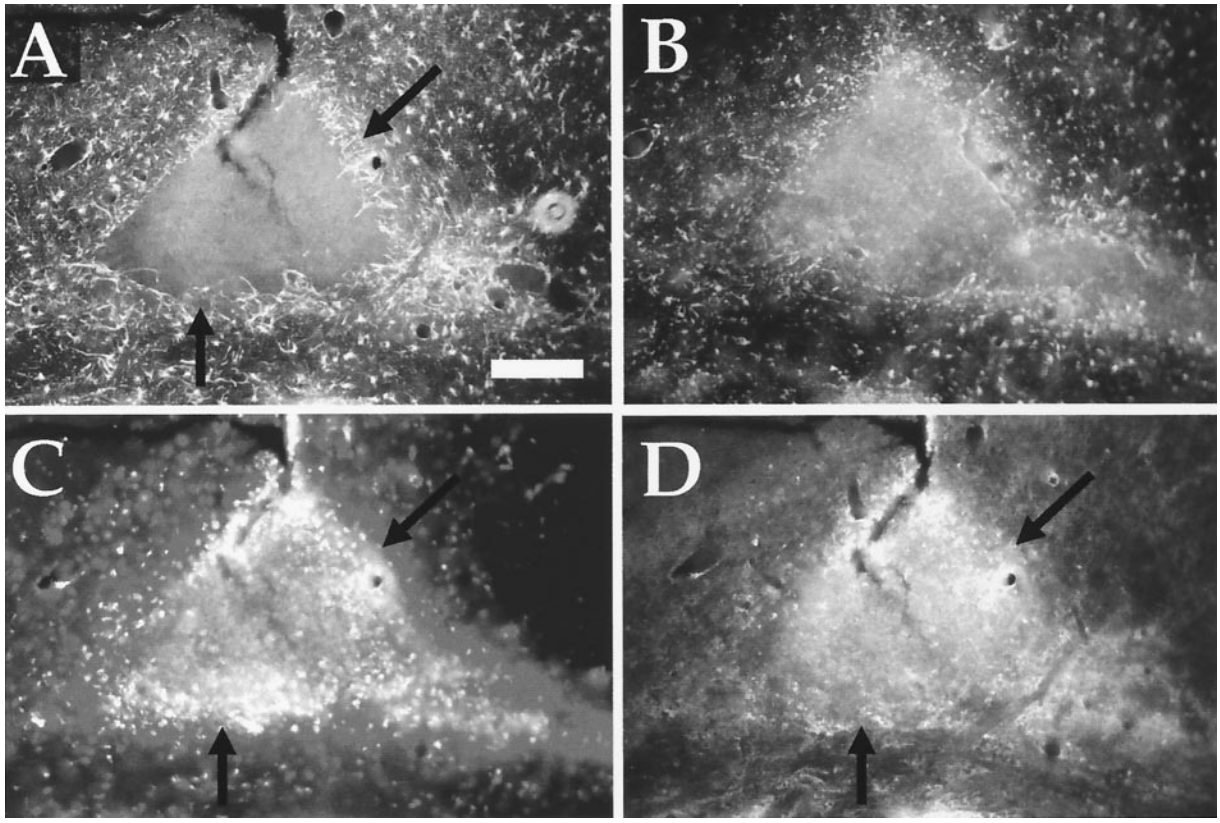

Figure 5. Representative zymosan-induced cavities, inflammation, and proteoglycan upregulation at 3 d after microinjection *in vivo*. Astrocyte GFAP staining (*A*) and vimentin intermediate filament staining (*B*) demarcate the astrocyte-free cavity that is filled with activated macrophages and microglia (*C*). These inflammatory infiltrates are associated with increases in proteoglycans (*D*), especially at the borders of the developing cavity (*arrows*; *A*, *C*, *D*). Scale bar, 225 μm.

As a control for the injection procedure, microinjections of 0.5 μl of saline at the four time points did not lead to increased cavity size over the 2 week experimental period (Figs. 1*E–H,* 2), demonstrating that physical aspects of the injection protocol were not sufficient to lead to cavitation. As an additional particulate control, 0.5 μl of latex microspheres 3 μm in diameter (the same size as zymosan particles and at the same concentration) was injected and analyzed at the four time points and also did not lead to significant increases in cavity size from initial injection to 2 weeks (Figs. 1*I–L*, 2), demonstrating that zymosan-induced inflammatory cavitation is a specific secondary effect that is not reproduced by merely the presence of foreign particles of this size in the brain.

Particulate macrophage activator *in vivo* leads to cavitation, inflammation, and putative inhibitory molecule production within white matter

The areas of corpus callosum devoid of astrocytes at 3 d after zymosan injection (Fig. 3*A*) were associated with axonal destruction in the region of developing cavitation (Fig. 3*B*). Thus, large numbers of damaged and dystrophic-appearing axon ends with enhanced neurofilament immunostaining were found at the borders of the enlarging cavities and sometimes within the cavities themselves (Fig. 3*C,D*, *arrows*). These pathological axon changes were not found after control saline injections and were minimal after latex bead injections. Importantly, the damage done to axons by the process of cavitation was irreparable even though filling in of the wound cavity by astrocytes and blood vessels had occurred. Thus, the borders of the initial cavity demonstrated by the damaged neurofilament-containing axons at 3 d (Fig. 3*B*) remained large at 2 weeks and did not fill in even with the return of astrocytes into the lesion (Fig. 3*E,F*). Compare the dramatic areas of inflammatory axon damage after 3 d (Fig. 3*B*) and 2 weeks (Fig. 3*F*) with the minimal amount of direct damage evident immediately after zymosan injection (Fig. 3*G*).

The *in vivo* microinjection of sterile zymosan particles led to a rapid development of intense inflammation with dense accumulations of activated macrophages and microglia observed with the ED1 antibody at the site of injection at 3 d (Fig. 4*A*). The activated inflammatory infiltrates identified by ED1 immunostaining were diminished by 1 week (Fig. 4*B*) and by 2 weeks were even further diminished (Fig. 4*C*). Although a modest number of inflammatory cells was associated with the needle tracts of all injections, the dense accumulations of macrophages and microglia found with a single injection of zymosan were not observed with single injections of saline, latex beads, or LPS.

The large inflammation-induced cavities that developed 3 d after zymosan injection were devoid of astrocyte GFAP staining (Fig. 5*A*) and vimentin staining (Fig. 5*B*) and were filled with dense accumulations of activated macrophages and microglia (Fig. 5*C*) that were closely associated with areas of tissue demonstrating increased levels of chondroitin sulfate proteoglycans (Fig. 5*D*), particularly at the borders of the developing cavities (Fig. 5*A,D*, *arrows*). The astrocyte-free cavities, which persisted at 1 week after injection (Fig. 6*A*), contained high levels of proteoglycan immunoreactivity inside and at the borders of the cavities (Fig. 6*A,B*, *white arrowheads*). At 1 and 2 weeks after zymosan

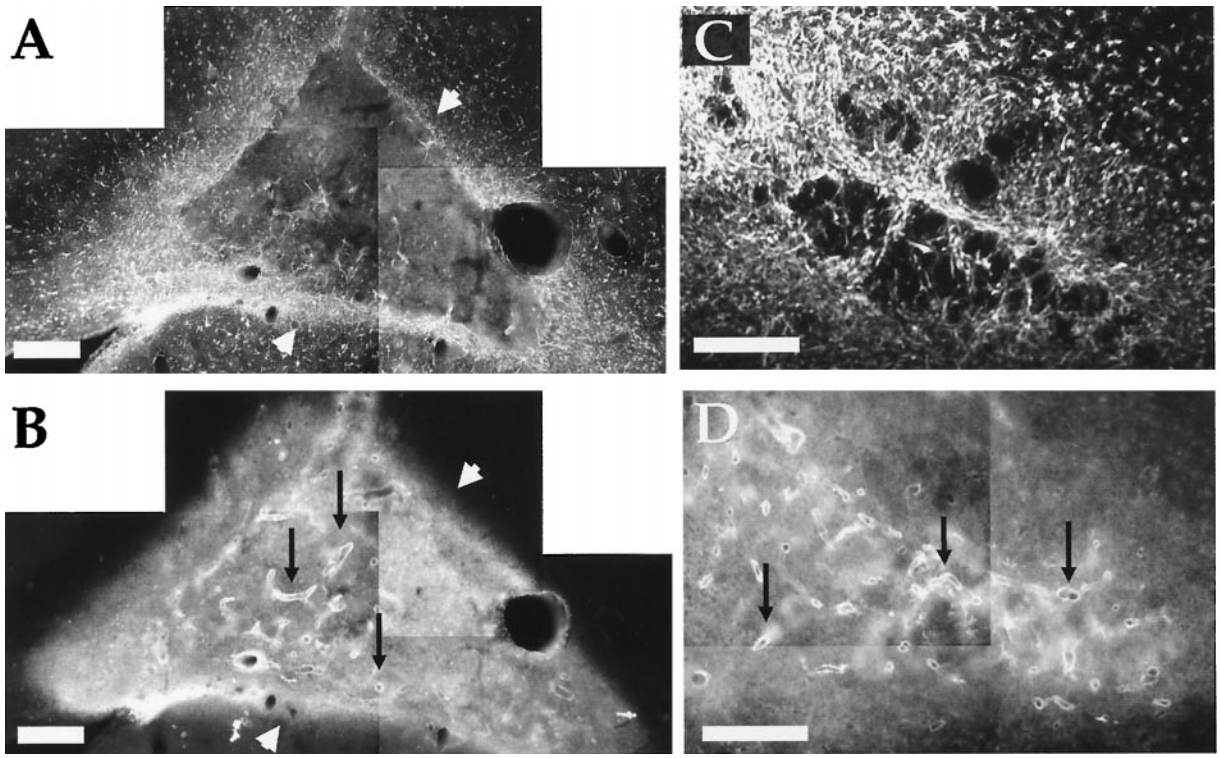

Figure 6. Analysis of zymosan microinjection sites *in vivo* at 1 week (*A, B*) and 2 weeks (*C, D*) using double-immunostaining techniques to visualize GFAP (*A, C*) and chondroitin sulfate proteoglycans (*B, D*). Note the increases in proteoglycans associated with the borders of the cavity (*A, B; white arrowheads*) and the intense upregulation of proteoglycan staining associated with blood vessels within the cavity at 1 week (*B; black arrows*) and 2 weeks (*D*; *black arrows*; higher power). Intensely GFAP+ astrocytes have repopulated and filled in the cavity at 2 weeks in *C* (higher power), which reduces the cavity size to control levels found immediately after injection (see Fig. 2). Scale bars, 250 μm.

injection, increases in proteoglycans were found immediately surrounding structures resembling blood vessels within the heart of the macrophage-filled cavity (Fig. 6*B,D*, *black arrows*), and staining for a marker of endothelial cells (RECA-1) demonstrated similar patterns of blood vessel staining in adjacent sections (data not shown). At 2 weeks after injection, astrocytes began to repopulate the cavity (Fig. 6*C*), which led to a statistically smaller cavity area at this time point (see Fig. 2). Single injections of latex beads, saline, or LPS did not lead to dramatic increases in proteoglycans, although the immediate site of injection and the needle tract itself did demonstrate local production of proteoglycans.

Activated microglia and macrophages *in vitro* are detrimental to adult neurons

Cocultures of microglial cells in direct contact with adult DRG neurons demonstrated that in comparison with nonactivated microglia, zymosan-activated microglia significantly lowered the survival of DRG neurons after 24 hr and 3 d (Fig. 7*A*). Similarly, peritoneal macrophages activated with zymosan also significantly lowered the number of live adult DRG neurons when compared with coculture with nonactivated macrophages (Fig. 7*B*).

To determine whether the detrimental effects of activated microglia and/or peritoneal macrophages on adult neurons could be modulated by their association with growth-supportive astrocytes, we conducted experiments to examine the effects of zymosan-activated inflammatory cells on neurons growing on astrocyte monolayers. These experiments showed similar reductions in adult neuron survival with activated microglial cells or macrophages even in the presence of an astrocyte substrate (Fig. 7*C,D*), demonstrating that the presence of astrocytes was not sufficient to attenuate the detrimental effects on neuron survival.

Activated macrophages *in vitro* lead to progressive cavitation of astrocytes

Interestingly, both activated microglial cells and activated peritoneal macrophages also appeared to have striking morphological effects on the astrocyte monolayers themselves, in addition to their detrimental effects on neurons in the coculture experiments. Although the astrocyte effects were not quantified in this initial experiment, the cellular responses leading to astrocyte-free areas of the cultures may model some relevant biological aspects of the process of progressive cavitation *in vivo*. Therefore, we developed an *in vitro* model to determine whether macrophages activated with zymosan were sufficient to induce the development of astrocyte-free cavities in tissue culture.

Our tissue culture model of cavity formation compared the reactions of astrocytes in established confluent monolayers with the introduction and direct interaction with activated or nonactivated macrophages, similar to the sequence of events after trauma in the nervous system. Quantitative measurements were taken to evaluate the integrity of the astrocyte monolayer after a 24 hr or 3 d inflammatory challenge by zymosan-activated or control nonactivated peritoneal macrophages. The areas of the culture that were covered previously by the initial confluent monolayer of astrocytes that then subsequently became devoid of cells after the coculture period were quantitatively measured and expressed as the area of "culture cavity" formation (see Fig. 8*E,F*). These cavities could result from astrocyte migration, astrocyte loss, or various combinations of processes.

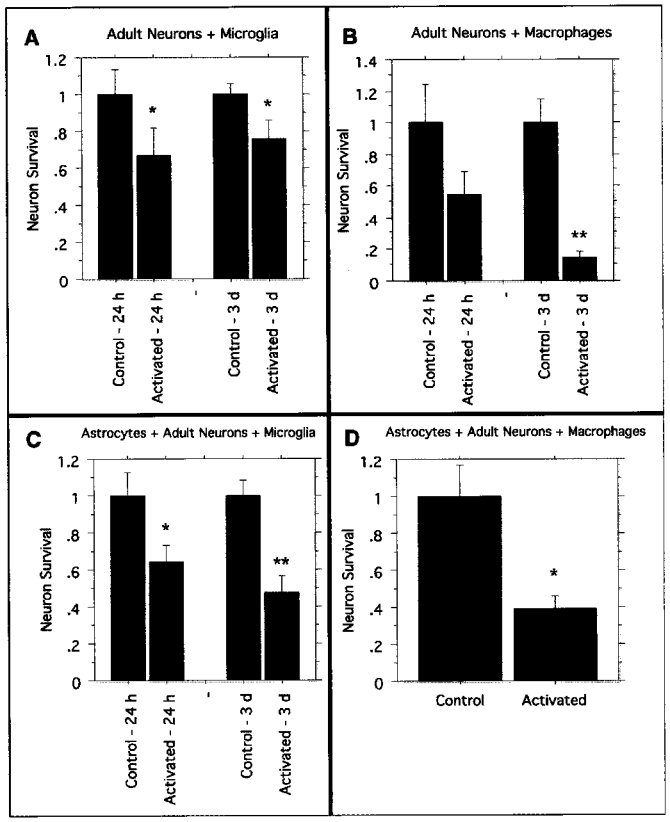

Figure 7. Activated microglial cells and activated peritoneal macrophages are detrimental to adult neurons in direct coculture conditions. *A,* The survival of adult DRG neurons is diminished by the presence of zymosan-activated microglial cells at 24 hr and 3 d in comparison with control nonactivated microglial cells (controls standardized to 1.0 in all *graphs*). *B,* Similarly, adult DRG neuron survival is compromised by the addition of activated peritoneal macrophages as compared with nonactivated macrophages. *C,* Growth of adult neurons on supportive astrocyte monolayers is not sufficient to prevent the loss of live neurons caused by activated microglial cells at 24 hr and 3 d of culture. *D,* Similarly, activated peritoneal macrophages added to adult neurons cultured on astrocyte monolayers lead to a significant loss of live neurons when compared with nonactivated macrophages at 24 hr of culture. Significance is relative to the control nonactivated macrophage preparations using the nonparametric Mann–Whitney *U* test, and *graphs* report group means ± SEM (*$p < 0.05$; **$p < 0.0001$).

Qualitatively, cocultures that contained zymosan-activated macrophages were strikingly different from those with nonactivated macrophages, in that astrocytes vacated large areas of the culture dish and the density of remaining astrocytes appeared to be increased. Computer-assisted image analysis was conducted to measure these cellular changes in representative low-power microscopic fields of view for each experiment. All comparisons were made between control astrocyte cultures with the addition of nonactivated macrophages and experimental astrocyte cultures with the addition of zymosan-activated macrophages. Statistical analysis demonstrated that the astrocyte area of culture cavitation was significantly increased with activated macrophages at 24 hr and at 3 d (Fig. 8*A*). Astrocyte density was significantly increased at 24 hr and slightly increased at 3 d (Fig. 8*B*), suggesting that astrocyte migration was a possible mechanism that led to cavitation in the cultures exposed to activated macrophages. The numbers of astrocytes were also decreased at both time points, which suggested that some astrocytes in the activated cultures may have died or perhaps may have changed their adhesive properties in response to the inflammatory stimuli and detached from the matrix either before or after culture fixation. To diminish the possibility of astrocyte detachment, experiments using more adhesive laminin-coated culture substrates were conducted, which demonstrated that when activated macrophages were added to astrocytes on laminin, the average area of culture cavities was also significantly increased and astrocyte density was increased. However, the number of astrocytes on this more adhesive substrate was unchanged, suggesting that astrocyte detachment was primarily responsible for the decreases in cell number seen in the other experiments. Control experiments demonstrated that zymosan treatment of astrocyte cultures in the absence of macrophages did not lead to significant changes in astrocyte number, the size of culture cavities, or astrocyte density.

To determine whether these effects on astrocytes might be mediated by soluble macrophage secretory products, experiments using media conditioned by nonactivated macrophages in comparison with media conditioned by zymosan-activated macrophages demonstrated results similar to those of the experiments conducted with live macrophages. Conditioned media from activated macrophages used for 3 d on astrocyte cultures with laminin substrates demonstrated significant increases in astrocyte cavity area (Fig. 8*C*), along with significantly increased astrocyte density and no changes in astrocyte number. Figure 8*C* illustrates the average astrocyte cavity area for three different sets of conditioned media experiments using 5×10^6, 10×10^6, and 12×10^6 macrophages per flask for conditioning the media. Higher numbers of macrophages in the conditioning media were associated with larger astrocyte cavities (Fig. 8*C*).

To characterize further the heat sensitivity or stability of the unidentified inflammatory factors in the activated macrophage–conditioned media that were leading to astrocyte cavitation, experiments were conducted using heated or boiled conditioned media on astrocytes growing on poly-L-lysine–coated substrates. Figure 8*D* illustrates that full-strength conditioned media from zymosan-activated macrophages caused astrocyte cavitation after 24 hr in culture when compared with astrocyte cultures with nonactivated macrophage–conditioned media. Mild heat treatment of 60°C for 15 min diminished the effect of the activated macrophage–conditioned media but did not completely prevent it. In other experiments, macrophage-conditioned media were used in a 1:1 dilution with fresh culture media. Zymosan-activated macrophage–conditioned media diluted 50% with fresh media were still sufficient to induce the astrocytes to form culture cavities, a result that was completely abolished by boiling the conditioned media before dilution with fresh media. These experiments suggest that the cavity-inducing factors present in the activated macrophage–conditioned media are sensitive to heat and boiling.

Two specific receptor agonists are required for cavity formation *in vitro*

Zymosan particles are composed of α-mannan and β-glucan residues (Lombard et al., 1994), and zymosan phagocytosis by macrophages involves the mannose receptor and/or the β-glucan lectin-binding site of the CR3 β2-integrin (Mac-1; CD11b/CD18) receptor present on macrophages (Xia et al., 1999). To address the issue of potential signaling mechanisms and cellular triggers for these effects, we used two separate receptor agonists in our *in vitro* cavitation assay to determine which receptors may be involved in the specific activation of macrophages to stimulate the

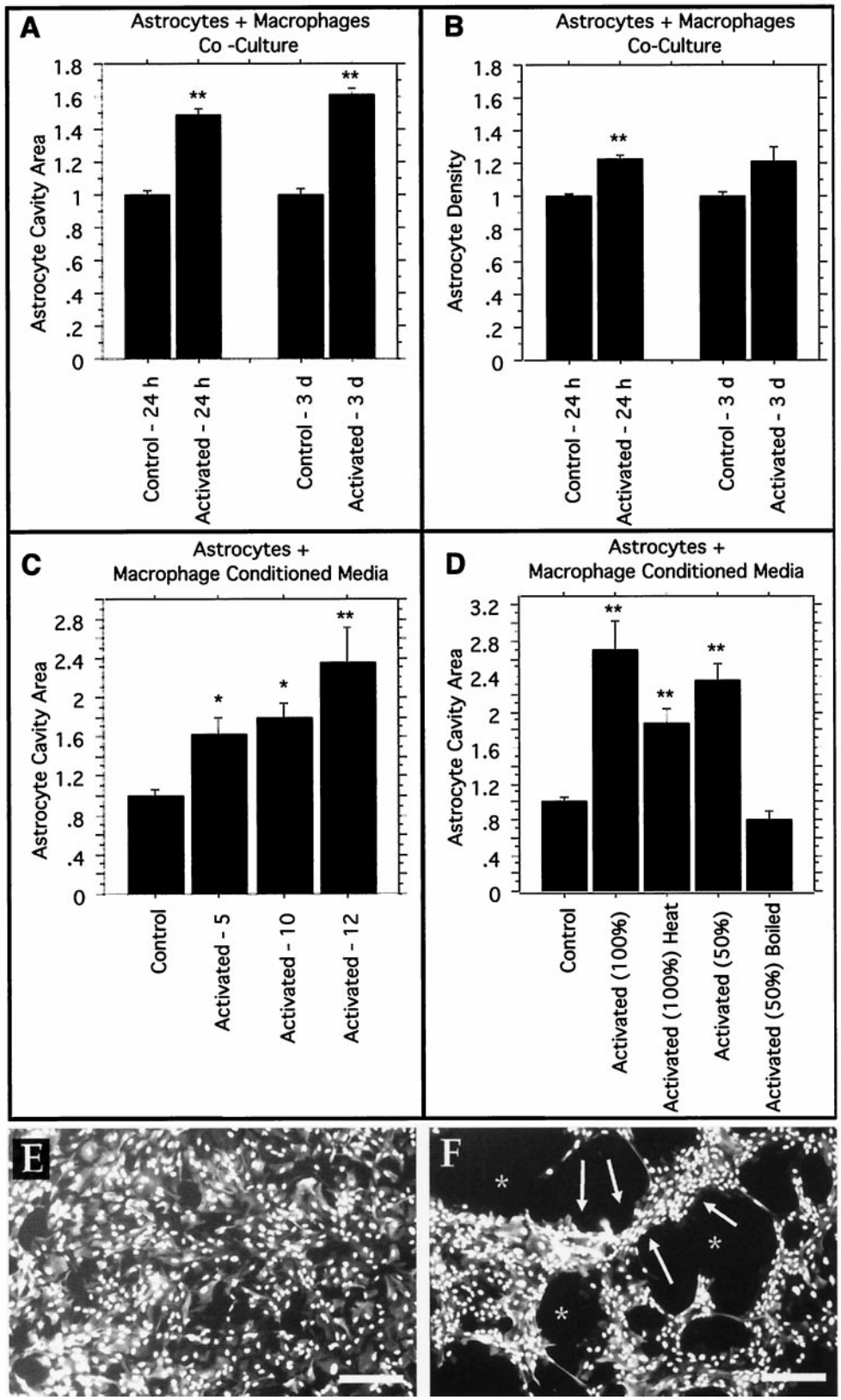

Figure 8. Inflammation leads to astrocyte cavitation in the *in vitro* astrocyte cystic cavitation model. The area of astrocyte cavity per microscopic field is significantly increased by activated macrophages or activated macrophage–conditioned media. *A, B*, Astrocytes + macrophages coculture. Astrocyte monolayers were established on poly-L-lysine coverslips, and peritoneal macrophages were added with no activating stimulant [control nonactivated macrophages (*Control*)] or with zymosan particles [activated macrophages (*Activated*)]. Control cultures are normalized to a value of 1, and all replicates are combined and expressed relative to their own individual controls. *A,* Astrocyte cavity area per field of view (areas of the culture that were covered previously by the confluent monolayer of astrocytes and that are subsequently devoid of cells). Significant increases at 24 hr ($p < 0.0001$) and 3 d ($p < 0.0001$) in the presence of activated macrophages as compared with nonactivated macrophages are shown. *B,* The density of astrocytes. A significant increase at 24 hr ($p < 0.0001$) and a slight increase at 3 d ($p = 0.0723$) suggest that astrocyte migration may be occurring in the cultures exposed to activated macrophages. *C, D*, Astrocytes + macrophage-conditioned media. Astrocyte monolayers were established with conditioned media from macrophage cultures, either zymosan-activated macrophages (*Activated*) or nonactivated control macrophages (*Control*). Control cultures are normalized to a value of 1. *C,* Cavity area of astrocyte monolayers grown on laminin in the presence of macrophage-conditioned media for 3 d with increasing numbers of macrophages present during the initial conditioning step (5×10^6, 10×10^6, and 12×10^6 macrophages per 10 ml of conditioned media). The significant cavity formation produced by activated macrophage–conditioned media is demonstrated. *D,* Cavity area of astrocyte monolayers grown on poly-L-lysine in the presence of macrophage-conditioned media for 24 hr with various treatments to the conditioned media. Full-strength conditioned media [*Activated (100%)*] lead to a significantly larger culture cavity ($p < 0.0001$), whereas heating that same full-strength media to 60°C for 15 min [*Activated (100%) Heat*] modestly decreases the cavitation, which is still significantly higher than that in control nonactivated macrophage–conditioned media that have been heated ($p < 0.0001$). Conditioned media diluted to 50% strength with fresh media [*Activated (50%)*] retain cavity-inducing activity ($p < 0.0001$), but boiling the conditioned media for 40 min before 50% dilution with fresh media [*Activated (50%) Boiled*] abolishes the effects. *E, F*, Representa-tive photomicrographs of as-trocyte cultures in the *in vitro* cavitation model stained with GFAP to visualize astrocyte intermediate filaments and with DAPI to visualize cell nuclei demonstrating a typical control (*E*; nonactivated macrophage–conditioned media from *C*) and a typical activated (*F*; activated macrophage–conditioned media from *C*). Note the even distribution of the astrocyte monolayer in *E*, whereas *F* contains areas of increased astrocyte density (*arrows*) and areas of culture cavity (*asterisks*). Similar results were seen with the cell coculture experiments reported in *A* and *B*. Scale bars, 225 μm. ANOVA with reported significance is relative to the appropriate control nonactivated macrophage preparation or conditioned media, and *graphs* report group means ± SEM (*$p < 0.005$; **$p < 0.0001$).

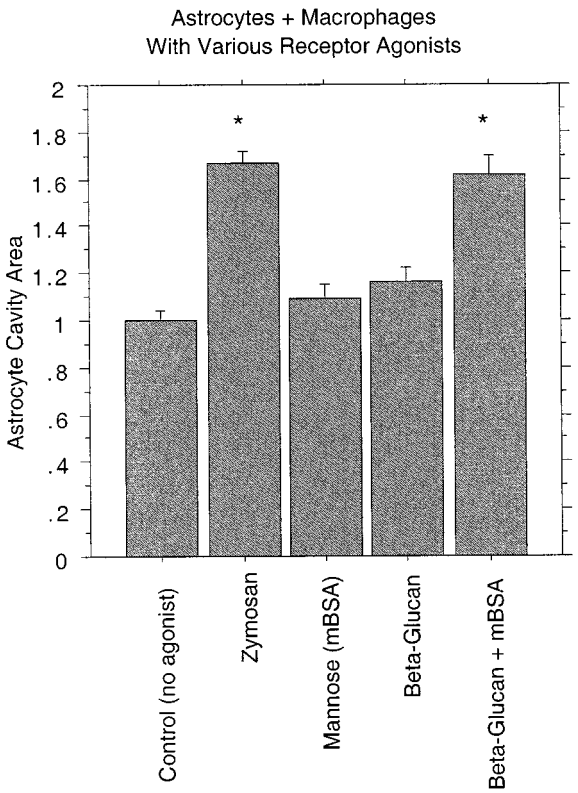

Figure 9. Simultaneous activation of both the macrophage mannose receptor and the β-glucan–binding site of CR3 on macrophages induces astrocyte cavitation in the *in vitro* astrocyte cystic cavitation model. Each receptor agonist category is expressed relative to simultaneous control (no agonist) nonactivated macrophage and astrocyte cocultures set to a value of 1, and all replicates are combined for each category. Astrocyte monolayers were established, and peritoneal macrophages were added with no activating stimulant [*Control (no agonist)*; nonactivated macrophages] or with various receptor agonists (zymosan, mBSA, β-glucan, or β-glucan + mBSA). Mannose receptor agonists alone (mBSA) or CR3 β-glucan site agonists alone (purified particulate β-glucan) were not sufficient to activate the macrophages to induce the formation of astrocyte cavities *in vitro*. However, addition of both mBSA and β-glucan simultaneously as macrophage activators in the macrophage and astrocyte coculture mimicked the development of astrocyte cavities induced by the zymosan stimulation of macrophages. ANOVA with reported significance is relative to the control (no agonist) nonactivated macrophage preparation or conditioned media, and the *graph* reports group means ± SEM (*$p < 0.0001$).

formation of astrocyte cavities in our system. Particulate β-glucan, a specific agonist for the β-glucan site of macrophage CR3 (Thornton et al., 1996), and mBSA, a specific high-affinity agonist for the mannose receptor of macrophages (Wileman et al., 1986; Engering et al., 1997), were used in the place of zymosan as potential macrophage activators. In these experiments, the particulate macrophage activator β-glucan was used at 0.05 mg/ml alongside simultaneous cultures with zymosan at 0.05 mg/ml, and mBSA was used at 1 μM, a concentration slightly higher than the maximum demonstrated to activate macrophages fully in another model (Gelderman et al., 1998). Separate control experiments demonstrated that astrocytes by themselves treated with mBSA alone, β-glucan alone, or mBSA + β-glucan were not significantly affected in any of the categories tested, particularly important controls in view of the recent report that, for the first time, describes mannose receptor expression by astrocytes themselves (Burudi et al., 1999). However, these control experiments indicated that the mannose receptor ligand (mBSA) with or without β-glucan particles did not induce any significant astrocytic changes in the absence of macrophages.

As illustrated in Figure 9, mBSA-activated macrophages were not sufficient to increase the cavity area significantly. Similarly, β-glucan–activated macrophages were not sufficient to increase the cavity area significantly. However, simultaneous stimulation of macrophages with both mBSA and β-glucan in coculture with astrocytes mimicked the zymosan activation experiments by increasing the astrocyte cavity area significantly. Therefore, stimulation of either the macrophage mannose receptor or the β-glucan site of CR3 alone is not sufficient to cause culture cavities, whereas concurrent stimulation of both receptors using these reagents does duplicate the results obtained with zymosan-activated macrophages.

Time-lapse recording of *in vitro* cavitation demonstrates astrocyte migration and morphological changes and suggests one mechanism for axon injury

Analysis of the *in vitro* cavitation model using time-lapse imaging allowed direct observation of the cellular interactions and provided insights into the mechanisms of cavity formation. Recordings of control cultures with astrocytes and nonactivated macrophages showed relatively static cultures with only minor cellular movements. In striking contrast, during the recordings of cocultures of activated macrophages with astrocyte monolayers, numerous examples of rapidly enlarging cavities were observed, primarily a result of astrocyte movement, morphological changes, and surprisingly rapid cellular withdrawal behaviors. In the cultures with activated macrophages, astrocytes were observed to extend and withdraw cellular processes, migrate into tight bundles, crawl from the culture substrate onto the upper surfaces of other cells, and change shapes as the cavities in the culture dish enlarged. Numerous examples of enlarging cavities were seen throughout the cocultures as the astrocyte movements appeared to be random and with no apparent organization. Still-frame excerpts of one region from a session of time-lapse recording in an activated culture are presented in Figure 10*A*. Note the enlarging cavity in the center of the frame as the astrocytes withdraw from that region. Time-lapse analysis indicated that astrocyte migration and withdrawal are major mechanisms of astrocyte cavity formation in our *in vitro* model.

On the basis of the results of the astrocyte and macrophage coculture imaging, additional time-lapse movies were taken of adult DRG neurons growing on astrocyte monolayers in the presence of macrophages. The DRG neurons were allowed to extend neurites for 12 hr on top of astrocytes before inflammatory challenge by the addition of nonactivated or activated macrophages. Neurites were identified on the basis of the morphological characteristics of long and thin cellular processes that were never flat and could be traced back to round neuronal cell bodies that always were located on the top of the glial monolayer throughout the time-lapse analysis period. Control cultures of adult DRG neurons growing on astrocytes in the presence of nonactivated macrophages again demonstrated relatively static cultures with only minor cell movements during the observation periods. However, in the series of time-lapse images with activated macrophages, striking observations were made of astrocytes abandoning the overlying adult DRG neurites while neuronal processes were stretched, moved, pulled, and even torn or dislodged as the astrocytes migrated to create cavities in the culture dish. Figure 10*B* presents a series of still-frame excerpts of a

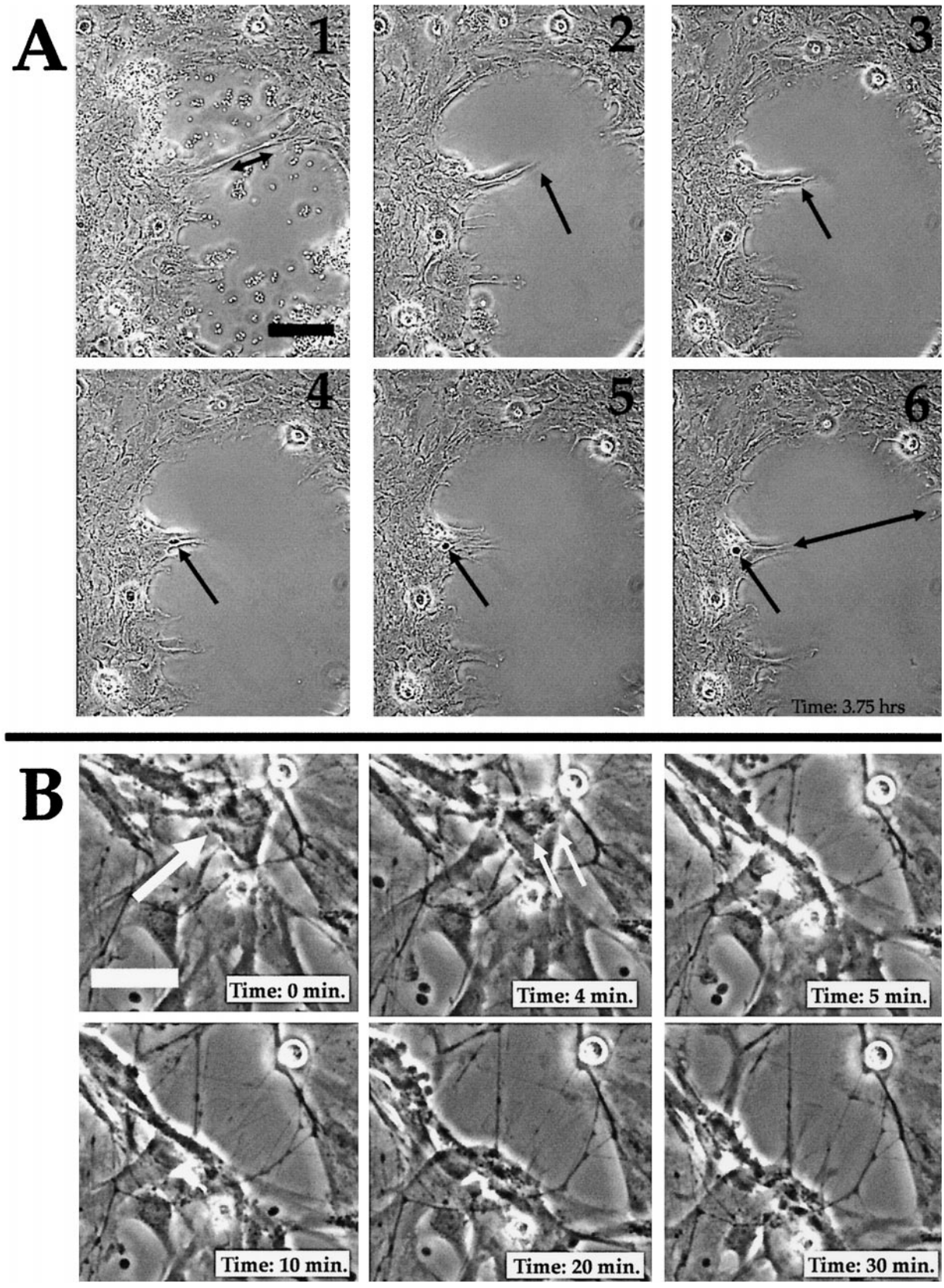

Figure 10. Time-lapse video analysis of the *in vitro* cavitation model. *A,* Selected *panels* from time-lapse video analysis of a developing astrocyte cavity in an astrocyte and zymosan-activated macrophage coculture. Intervals of 45 min separate each *panel* (*1–6*) for a total recording time of 3.75 hr. Note the *double-headed arrows* in *panels 1* and *6* that demarcate the width of the cavity at this location for each time point, illustrating the increase in cavity size at that point from ~80 to 200 μm over the observed time period. *Arrows* track a single astrocyte as it is stretched until it is broken or dislodged (*panel 2*), gradually moves up from the surface of the culture plate (*panels 3, 4*), and migrates back on top of the astrocyte monolayer (*Figure legend continues*)

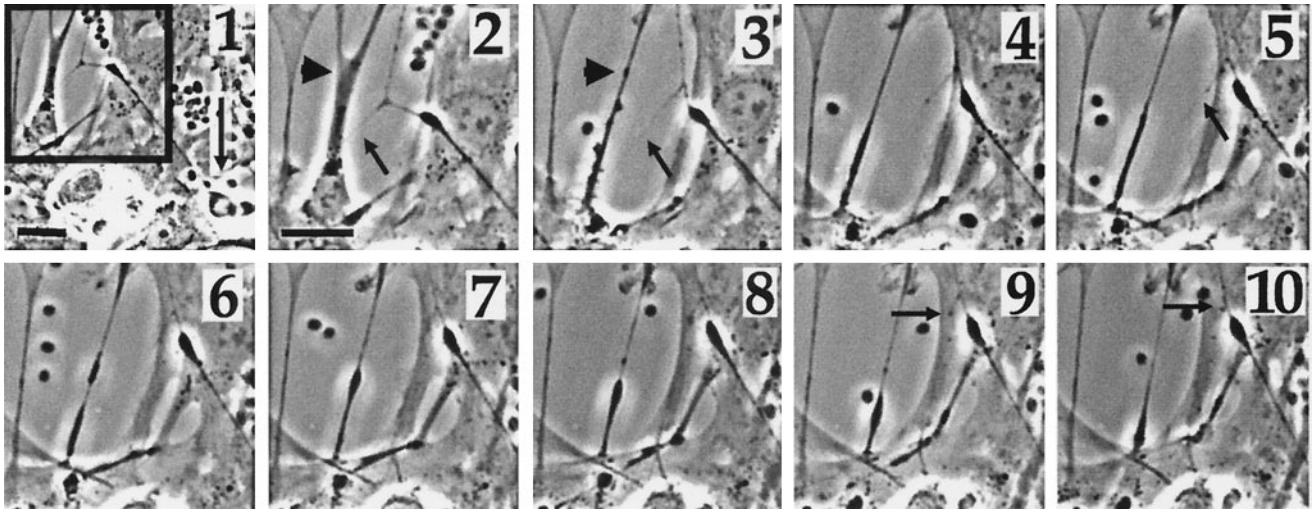

Figure 11. Selected *panels* from time-lapse video analysis demonstrating that astrocyte movements can have dynamic effects on neuron processes during astrocyte abandonment and cavity formation. An interval of 6 min separates each *panel* for a total recording time of 54 min. *Panel 1* is a low-power view of an adult DRG neuron (*arrow*) with a process (*boxed area*) that can be followed at higher power in *panels 2–10*. Note especially the astrocyte marked with an *arrowhead* and the bifurcated neurite marked with an *arrow* in *panels 2* and *3*. As this astrocyte cavity gradually increases in size, the marked astrocyte is pulled and stretched to a very thin morphology, whereas the marked neurite is broken or pulled free from its original connection in *panel 3* and is left to retract in *panels 4–10*. Note the retracting end of the neurite that is being reabsorbed in *panels 9* and *10* (*arrows*). This is a dramatic demonstration of the potential for neurite damage seen several times in our time-lapse analysis simply because of the physical processes of astrocyte movement and withdrawal. Scale bar, 40 μm.

rapidly developing astrocyte cavity in which neurites that had been associated with the upper surfaces of astrocytes are suddenly exposed and dynamically stretched across the new cavity. In particular, note the transition between 4 and 5 min in Figure 10*B* as a cavity rapidly develops where none existed previously, illustrating the sometimes rapid time course of astrocyte abandonment of neuronal processes within the activated macrophage cultures. Figure 11 demonstrates still-frame excerpts from a session of time-lapse recording of activated cultures in which the astrocyte movements directly impacted a neuron process. Figure 11 shows a single neurite as it was dislodged or broken as the astrocyte withdrawal pulled in the opposite direction, demonstrating the potentially destructive mechanical forces that such astrocyte movements can exert on neurites. These observations of dynamic cellular interactions between astrocytes and neuron processes suggest a mechanism for neurite movement and possible injury attributable to mechanical movements of astrocytes in response to inflammatory infiltrates.

Activated macrophages *in vitro* stimulate production of proteoglycans by astrocytes

Because *in vivo* inflammatory events are associated with increases in proteoglycan production (Figs. 5, 6), we looked for similar increases in chondroitin sulfate proteoglycans in our *in vitro* model of progressive cavitation. Astrocytes alone, astrocytes with zymosan alone, astrocytes with nonactivated macrophages (Fig. 12*A*), and astrocytes with nonactivated macrophage–conditioned media exhibited uniform low levels of proteoglycan staining and did not demonstrate any dramatic increases in proteoglycan throughout the culture. Interestingly, increased proteoglycan staining of individual astrocytes in a heterogeneous manner was found throughout the astrocyte cultures treated with zymosan-activated macrophages or in astrocyte-only cultures grown with activated macrophage–conditioned media (Fig. 12*B*). Examination of single cells at high power demonstrated that some astrocytes exhibited increased proteoglycan staining while others in close proximity did not (Fig. 12*C–F*).

Anti-inflammatory PPAR-γ agonists prevent *in vitro* cavity formation

On the basis of our results demonstrating the role of inflammatory activation of macrophages in the development of astrocyte cavitation in our *in vitro* model, we hypothesized that blocking the inflammatory activation would prevent these effects. Therefore, we tested anti-inflammatory agents that act as agonists to PPAR-γ for their ability to inhibit the formation of cavities in our *in vitro* cavitation assay. Astrocyte monolayer cultures on poly-L-lysine coverslips coated with laminin were maintained in coculture for 3 d with 100,000 macrophages and one of three drug treatments or vehicle control. Each group had two components

←

(*panel 5*) where it remains as a loosely attached ball (*panel 6*). Presumably, loosely attached cells such as this one would be subsequently lost into the liquid phase of the culture media either before or after culture fixation. *B,* Time-lapse video analysis of a rapidly appearing astrocyte cavity that exposes, stretches, and exerts force on overlying neurites that were abandoned by the supportive astrocyte substrate in an astrocyte, adult DRG neuron, and zymosan-activated macrophage coculture. Elapsed time is indicated in the *lower right-hand corner* of each *panel*. Note the astrocyte at 0 and 4 min that is undergoing mitosis (*large arrow; 0 min*) with the clearly visible separating chromosomes (*small double arrows; 4 min*). This single cell apparently occupies a key location for holding the local astrocyte meshwork together, as demonstrated at 5 min when this single cell has completed dividing and the astrocyte networks on either side rapidly pull apart leaving a cavity that continues to grow from 5 to 30 min. Neurites from the adult DRG neurons are growing throughout this area of the culture and are exposed across this cavity by the astrocyte withdrawal and subsequent cavity formation. Note the dynamic movements of the neurites after the astrocyte abandonment as they are pulled and stretched by the astrocytes on either side of this developing cavity. Scale bars: *A*, 100 μm; *B*, 40 μm.

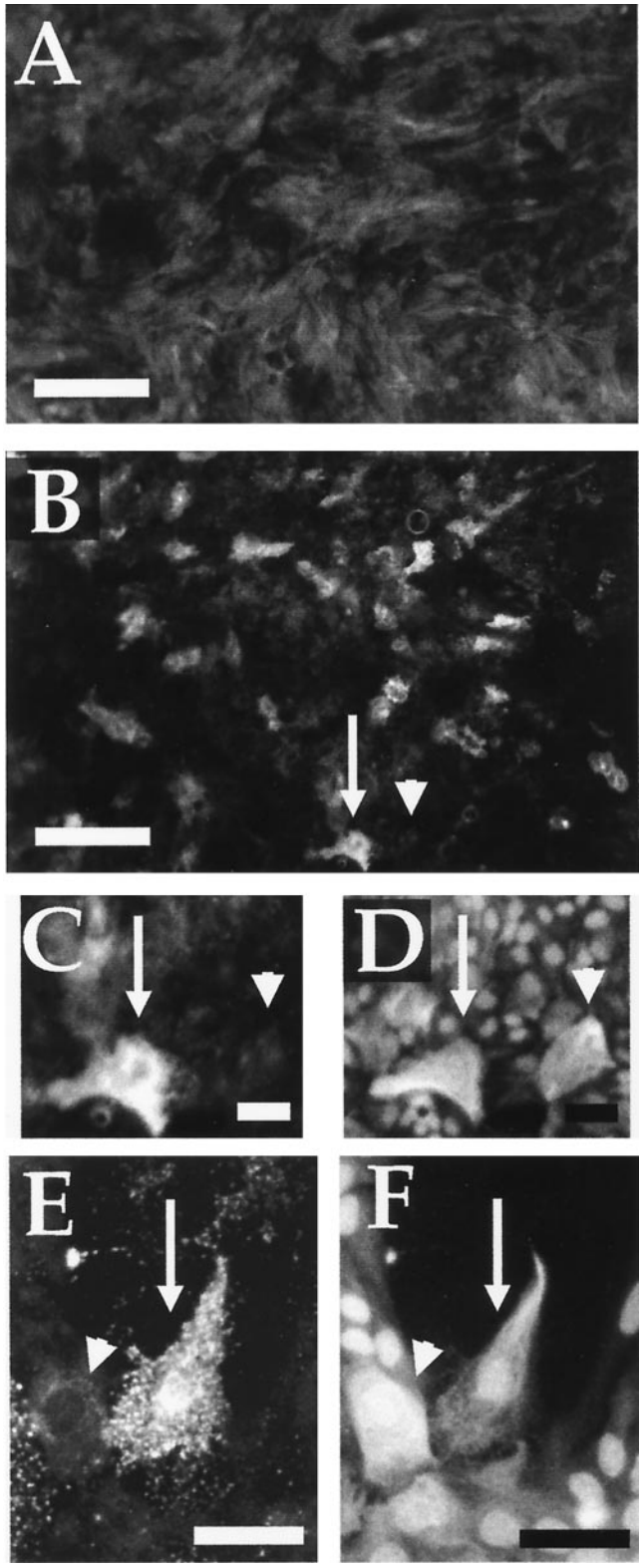

Figure 12. Inflammation *in vitro* leads to heterogeneous increases in proteoglycans in astrocyte cultures. Areas of the *in vitro* cavitation model were stained for chondroitin sulfate proteoglycans (*A–C, E*) or GFAP (*D, F*). *A*, Astrocytes with nonactivated macrophages demonstrate a uniform low level of proteoglycan staining in control cultures, a result that is also seen in astrocyte cultures with zymosan only or with nonactivated macrophage–conditioned media (data not shown). *B–D*, In contrast, individual cells with increased levels of proteoglycans can be observed in astrocyte cultures containing activated macrophages (data not shown) or in astrocyte-only cultures with activated macrophage–conditioned media (*B*). The *arrow* and *arrowhead* in *B* indicate two astrocytes shown in high power in *C* (proteoglycan) and *D* (GFAP). One astrocyte has increased proteoglycan staining (*arrow*), whereas the other nearby astrocyte has no such increase (*arrowhead*). *E, F*, High-power view is shown of two astrocytes (*arrow* and *arrowhead*) in which one has increased proteoglycan staining (*E*) whereas the other does not in an astrocyte culture (GFAP in *F*) with activated macrophages. Scale bars: *A, B*, 210 μm; *C, D*, 40 μm; *E, F*, 60 μm.

(nonactivated macrophages with treatment and zymosan-activated macrophages with treatment) for standardization within each treatment group. The treatment groups included no treatment [vehicle only (DMSO at 1 μl/ml)], indomethacin treatment (100 μM), prostaglandin J2 treatment (10 μM), and ciglitazone treatment (50 μM) of the zymosan-activated macrophages. As demonstrated in Figure 13, the area of culture cavity was significantly increased by activated macrophages with no treatment (as seen in Fig. 8), and indomethacin treatment of the activated macrophages did not prevent this increase in the area of the culture cavity relative to control levels. Prostaglandin J2 treatment and ciglitazone treatment of the activated macrophages while interacting with the astrocyte cultures abolished the increases in the area of culture cavities relative to their control levels with nonactivated macrophages. These results further demonstrate the importance of inflammatory macrophage interaction in the formation of astrocyte cavities and suggest that PPAR-γ agonists are able to block the destructive inflammatory events that follow activation of the macrophages by zymosan, thus preventing the subsequent astrocyte reactions leading to cavities in our *in vitro* model.

DISCUSSION

These experiments demonstrate the destructive effects of inflammation in the CNS by separating pathology caused by physical trauma from deleterious changes in response to inflammatory processes using models of postinjury progressive cavitation. Persistent inflammation in the absence of significant physical damage within CNS white matter can result in an expanding astrocyte-free cavity surrounded by glial scarring and extracellular matrix proteoglycans and the secondary destruction of axons. Activation of macrophages in our novel culture model of cavitation stimulated astrocyte reactions leading to dynamic migration, cavity formation, and astrocyte abandonment of neuronal processes, which suggests that a mechanical component may contribute to neurite damage. Our *in vitro* model identified the macrophage mannose receptor and β-glucan lectin site of the CR3 integrin receptor as important in inducing the macrophage state leading to astrocyte cavitation. We also demonstrated the therapeutic potential of anti-inflammatory treatments with agonists to PPAR-γ to prevent inflammation-induced astrocyte cavitation in our culture model.

Persistent inflammation in the absence of significant damage replicates postinjury secondary pathology

Our *in vivo* model of progressive cavitation minimized direct physical trauma while maximizing inflammatory activation by careful delivery of minute volumes of concentrated zymosan particles into the CNS. The intense inflammatory responses led to the rapid development of astrocyte cavities by a process that may model cavitation after traumatic injury (Windle et al., 1952; Balentine, 1978; Noble and Wrathall, 1985; Guth et al., 1994;

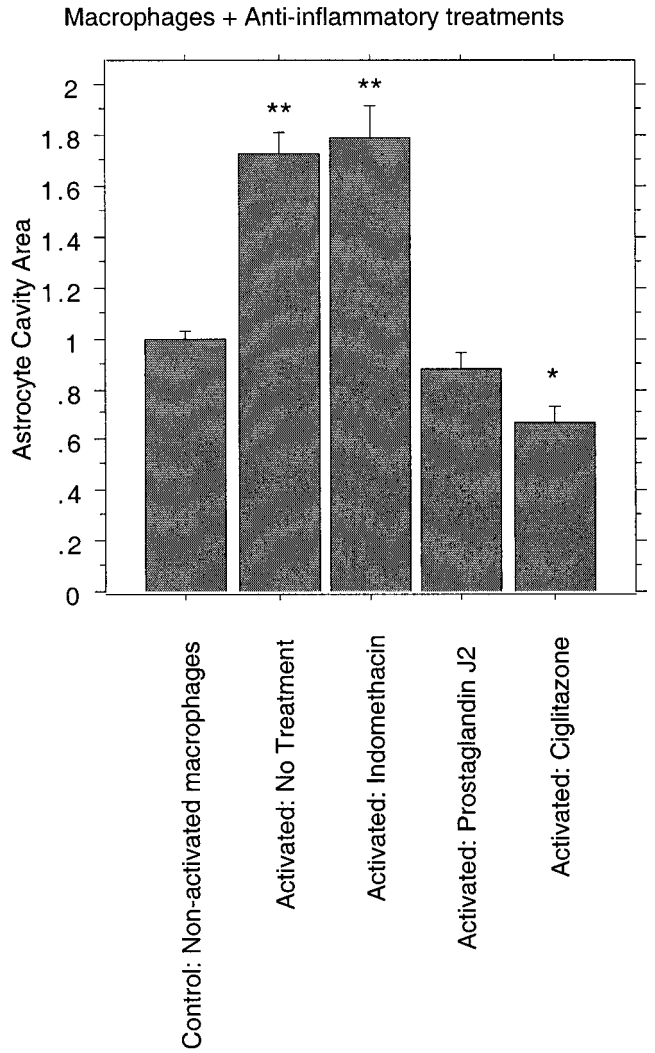

Figure 13. Quantitative analysis of the changes in astrocyte and macrophage cocultures by activation of macrophages and treatment with anti-inflammatory PPAR-γ agonists. Each treatment category is expressed relative to the appropriate drug- or vehicle-treated nonactivated macrophage control, with the average for each control group being set to 1 and all replicates being combined in each category. The area of astrocyte cavity per microscopic field is significantly increased by activated macrophages with no treatment (vehicle), which is analogous to the cavitation found after an *in vivo* CNS injury. Indomethacin treatment (100 μM) of the zymosan-activated macrophages does not prevent this increase in the area of the culture cavity relative to control levels. Prostaglandin J2 treatment (10 μM) and ciglitazone treatment (50 μM) of the zymosan-activated macrophages while interacting with the astrocyte cultures abolish the increases in the area of culture cavities relative to their control levels with nonactivated macrophages. ANOVA with Fisher's PLSD statistical significance is relative to the pooled *Control*: *Nonactivated macrophages* category ($^*p < 0.0005$; $^{**}p < 0.0001$).

Fitch and Silver, 1997a; Zhang et al., 1997). Secondary pathology in our inflammatory model mimicked the sequelae of CNS injury, such as increases in molecules associated with regenerative failure (Laywell et al., 1992; Levine, 1994; Fitch and Silver, 1997a). Proteoglycan upregulation in blood vessels is consistent with the increased vascularity within lesions (Blight, 1991b; Bartholdi et al., 1997) and the expression of syndecan in capillary endothelia during healing (Elenius et al., 1991; Wight et al., 1992). Our results support others suggesting similar destructive secondary inflammatory phenomena (Blight, 1985, 1994; Giulian and Robertson, 1990; Hirschberg et al., 1994; Popovich et al., 1994; Zhang et al., 1997; Weldon et al., 1998; Fitch and Silver, 1999b).

Specific and persistent macrophage activation induces cavity formation

A persistent macrophage stimulus was closely associated with the induction of the cascade of cellular events leading to *in vivo* astrocyte cavitation and axon damage. Zymosan stimulated a vigorous inflammatory response for days to weeks, presumably because of the insoluble nature of the particles remaining at the injection site. LPS, in contrast, is a soluble immunostimulant unable to initiate the cavitation cascade after a single injection in this study and others (Andersson et al., 1992; Montero-Menei et al., 1994), possibly because of its diffusible nature. In support of this idea, chronic inflammation from continuous LPS infusion does lead to cavitation (Szczepanik et al., 1996). The specificity of zymosan as an *in vivo* inflammatory activator was highlighted by the inability of control latex microspheres to initiate cavitation.

Zymosan contains α-mannan and β-glucan, and phagocytosis involves the mannose receptor and/or the β-glucan site of CR3 (Stewart and Weir, 1989; Ross and Vetvicka, 1993; Lombard et al., 1994; Xia et al., 1999). In our model, zymosan-activated macrophages induced changes in astrocytes that mimicked cavity formation after CNS injury. This was duplicated by simultaneous stimulation of the macrophage mannose receptor and the CR3 β-glucan site, whereas agonists to either receptor alone did not generate this response. Such costimulation and coincident signaling through multiple receptors have been highlighted as important in the immune system (Weintraub and Goodnow, 1998). In some cases, ligand binding to distinct receptors activates the integrin CR3 itself and enhances its affinity (Hazenbos et al., 1993; Schnitzler et al., 1999), and such "inside out" signaling requires kinase activity (Rabb et al., 1993; Hazenbos et al., 1995). Functional links between the mannose receptor family and other receptors have been suggested (McKay et al., 1998), and although the signaling pathway of the mannose receptor is unknown, it involves calcium flux (Marodi et al., 1993) and tyrosine kinase activation (Murai et al., 1996). The underlying pathways behind a potential functional link between the CR3 and mannose receptors remain to be elucidated.

Specific factors produced by activated macrophages that are responsible for astrocyte cavitation are unknown. Astrocyte clearing throughout our cultures suggests that these factors can lead to widespread migration, in contrast to movements away from a central source of *in vivo* inflammation. Our conditioned media experiments indicated that these factors are secreted, soluble, and heat sensitive, suggesting that they are distinct from neurotoxic factors secreted by activated microglia that are heat stable (Giulian et al., 1993a,b).

Highlighting the importance of the variable activation state of inflammatory cells, macrophages or microglial cells may benefit axon sprouting in some situations (Lazarov-Spiegler et al., 1996; Prewitt et al., 1997; Rabchevsky and Streit, 1997; Streit et al., 1998; Batchelor et al., 1999). In view of the apparent importance of the type of activation state in determining whether inflammation has positive or detrimental effects, an intriguing question remains about the identity of physiological ligands for the mannose receptor and the CR3 *in vivo* and what additional receptors may be important for activating the destructive form of inflammation. Substances potentially found in areas of trauma that can bind to the CR3 and mannose receptors include infectious organisms, lysosomal enzymes, tissue plasminogen activator, red blood

cells, factor X, complement protein iC3b, and fibrinogen (Muller et al., 1983; Ross et al., 1985; Stewart and Weir, 1989; Taylor, 1993; Ishihara et al., 1998; Issekutz et al., 1999).

Astrocyte migration is a contributing factor to progressive cavitation

Delayed cell death after CNS injury is documented as one mechanism of secondary pathology leading to glial and neuronal cell loss and cavitation (Crowe et al., 1997; Liu et al., 1997; Conti et al., 1998). Although a small amount of cell death was observed in our cultures, time-lapse analysis demonstrated that dramatic astrocyte movements, morphological changes, and migration may be another mechanism for cavitation. Astrocyte movements, in turn, may lead to rapid abandonment of axons, thereby leaving them vulnerable to inflammatory damage, whereas stretching forces generated by astrocyte migrations may even contribute directly to axon damage.

Proteoglycans may be involved with cell migration during cavitation

Proteoglycan increases previously described surrounding cavities *in vivo* (Figs. 5, 6) (MacLaren, 1996; Fitch and Silver, 1997a) were also demonstrated *in vitro* by astrocytes stimulated to change their motility and morphological characteristics in coculture with activated macrophages or conditioned media. This heterogeneous increase in chondroitin sulfate proteoglycan may be related to the astrocyte migration and adhesive changes seen in our time-lapse analysis, as proteoglycans have been implicated previously in cell motility and migration (Kinsella and Wight, 1986; Faassen et al., 1992; Wight et al., 1992; Grumet et al., 1993; Faber-Elman et al., 1996; Gary et al., 1998).

This highlights an interesting paradox concerning proteoglycans, because it is also well established that proteoglycans are capable of inhibiting axon regeneration (Snow et al., 1990; McKeon et al., 1991; Dou and Levine, 1994). Although migration of progenitor cells occurs within the proteoglycan-rich extracellular matrix of the subventricular zone (Gates et al., 1995; Thomas et al., 1996; Alvarez-Buylla and Temple, 1998), glial cell matrix molecules also serve as boundaries for axon growth during development and regeneration (for review, see Fitch and Silver, 1997b). A similar phenomenon was documented here; astrocytes and endothelial cells repopulated the proteoglycan-filled cavities after 2 weeks, whereas no axon growth into this area was observed. These contrasting reactions suggest fundamental differences between the mechanisms of axon regeneration and cellular migration.

Treatments that limit inflammatory factor transcription may have therapeutic effects after trauma

We used a class of broadly acting anti-inflammatory agents that act as agonists of the transcription factor PPAR-γ to test our hypothesis that blocking inflammatory activation would prevent cavitation in our culture model. The PPARs are a steroid hormone receptor superfamily of transcription factors that, when activated, lead to gene activation or repression. PPAR-γ is a potent negative regulator of macrophage activation, and agonists to this ligand-dependent transcription factor depress macrophage inflammatory expression (Jiang et al., 1998; Ricote et al., 1998). Some of this inhibition of macrophage inflammatory gene transcription appears to be a result of antagonizing the transcription factors NF-κB, AP-1, and the STATs (Ricote et al., 1998). NF-κB has been implicated previously as important for inflammatory damage after spinal cord injury (Bethea et al., 1998) and is stimulated in macrophages activated by β-glucan (Battle et al., 1998).

The potent PPAR-γ agonists ciglitazone and prostaglandin J2 effectively blocked the destructive effects of activated macrophages in our *in vitro* model of cavitation. These results suggest a potential therapeutic use for PPAR-γ agonists in the treatment of spinal cord and brain injuries to prevent the inflammatory sequelae leading to secondary damage. Insights into inflammatory cell activation via specific receptor pathways, the role of macrophages in tissue destruction, and ways to modify these reactions with anti-inflammatory agents will lead to therapeutic strategies designed to limit secondary pathology and promote CNS wound healing.

REFERENCES

Alvarez-Buylla A, Temple S (1998) Stem cells in the developing and adult nervous system. J Neurobiol 36:105–110.

Andersson PB, Perry VH, Gordon S (1992) The acute inflammatory response to lipopolysaccharide in CNS parenchyma differs from that in other body tissues. Neuroscience 48:169–186.

Anthony DC, Bolton SJ, Fearn S, Perry VH (1997) Age-related effects of interleukin-1 beta on polymorphonuclear neutrophil-dependent increases in blood-brain barrier permeability in rats. Brain 120:435–444.

Balentine JD (1978) Pathology of experimental spinal cord trauma. I. The necrotic lesion as a function of vascular injury. Lab Invest 39:236–253.

Bartholdi D, Rubin BP, Schwab ME (1997) VEGF mRNA induction correlates with changes in the vascular architecture upon spinal cord damage in the rat. Eur J Neurosci 9:2549–2560.

Batchelor PE, Libertore GT, Wong JYF, Porritt MJ, Frerichs F, Donnan GA, Howells DW (1999) Activated macrophages and microglia induce dopaminergic sprouting in the injured striatum and express brain-derived neurotrophic and glial cell line-derived neurotrophic factor. J Neurosci 19:1708–1716.

Battle J, Ha T, Li C, Della Beffa V, Rice P, Kalbfleisch J, Browder W, Williams D (1998) Ligand binding to the (1→3)-beta-D-glucan receptor stimulates NFkappaB activation, but not apoptosis in U937 cells. Biochem Biophys Res Commun 249:499–504.

Bethea JR, Castro M, Keane RW, Lee TT, Dietrich WD, Yezierski RP (1998) Traumatic spinal cord injury induces nuclear factor-κB activation. J Neurosci 18:3251–3260.

Blight AR (1985) Delayed demyelination and macrophage invasion: a candidate for secondary cell damage in spinal cord injury. Cent Nerv Syst Trauma 2:299–315.

Blight AR (1991a) Morphometric analysis of a model of spinal cord injury in guinea pigs, with behavioral evidence of delayed secondary pathology. J Neurol Sci 103:156–171.

Blight AR (1991b) Morphometric analysis of blood vessels in chronic experimental spinal cord injury: hypervascularity and recovery of function. J Neurol Sci 106:158–174.

Blight AR (1994) Effects of silica on the outcome from experimental spinal cord injury: implication of macrophages in secondary tissue damage. Neuroscience 60:263–273.

Burudi EME, Riese S, Stahl PD, Regnier-Vigouroux A (1999) Identification and functional characterization of the mannose receptor in astrocytes. Glia 25:44–55.

Conti AC, Raghupathi R, Trojanowski JQ, McIntosh TK (1998) Experimental brain injury induces regionally distinct apoptosis during the acute and delayed post-traumatic period. J Neurosci 18:5663–5672.

Crowe MJ, Bresnahan JC, Shuman SL, Masters JN, Beattie MS (1997) Apoptosis and delayed degeneration after spinal cord injury in rats and monkeys. Nat Med 3:73–76.

Davies SJ, Fitch MT, Memberg SP, Hall AK, Raisman G, Silver J (1997) Regeneration of adult axons in white matter tracts of the central nervous system. Nature 390:680–683.

Davies SJA, Field PM, Raisman G (1996) Regeneration of cut adult axons fails even in the presence of continuous aligned glial pathways. Exp Neurol 142:203–216.

Dou C-L, Levine JM (1994) Inhibition of neurite growth by the NG2 chondroitin sulfate proteoglycan. J Neurosci 14:7616–7628.

Ducker TB, Kindt GW, Kempe LG (1971) Pathological findings in acute experimental spinal cord trauma. J Neurosurg 35:700–707.

Elenius K, Vainio S, Laato M, Salmivirta M, Thesleff I, Jalkanen M (1991) Induced expression of syndecan in healing wounds. J Cell Biol 114:585–595.

Engering AJ, Cella M, Fluitsma D, Brockhaus M, Hoefsmit EC, Lanzavecchia A, Pieters J (1997) The mannose receptor functions as a high capacity and broad specificity antigen receptor in human dendritic cells. Eur J Immunol 27:2417–2425.

Faassen AE, Schrager JA, Klein DJ, Oegema TR, Couchman JR, McCarthy JB (1992) A cell surface chondroitin sulfate proteoglycan, immunologically related to CD44, is involved in type I collagen-mediated melanoma cell motility and invasion. J Cell Biol 116:521–531.

Faber-Elman A, Solomon A, Abraham JA, Marikovsky M, Schwartz M (1996) Involvement of wound-associated factors in rat brain astrocyte migratory response to axonal injury: in vitro simulation. J Clin Invest 97:162–171.

Fitch MT, Silver J (1997a) Activated macrophages and the blood brain barrier: inflammation after CNS injury leads to increases in putative inhibitory molecules. Exp Neurol 148:587–603.

Fitch MT, Silver J (1997b) Glial cell extracellular matrix: boundaries for axon growth in development and regeneration. Cell Tissue Res 290:379–384.

Fitch MT, Silver J (1999a) Beyond the glial scar: cellular and molecular mechanisms by which glial cells contribute to CNS regenerative failure. In: CNS regeneration: basic science and clinical advances (Tuszynski MH, Kordower JH, eds), pp 55–88. San Diego: Academic.

Fitch MT, Silver J (1999b) Inflammation and the glial scar: factors at the site of injury that influence regeneration in the central nervous system. In: Degeneration and regeneration in the nervous system (Saunders NR, ed). London: Harwood Academic, in press.

Freshney RI (1987) Culture of animal cells: a manual of basic techniques. New York: Wiley.

Gary SC, Kelly GM, Hockfield S (1998) BEHAB/brevican: a brain-specific lectican implicated in gliomas and glial cell motility. Curr Opin Neurobiol 8:576–581.

Gates MA, Thomas LB, Howard EM, Laywell ED, Sajon B, Faissner A, Gotz B, Silver J, Steindler DA (1995) Cell and molecular analysis of the developing and adult mouse subventricular zone of the cerebral hemispheres. J Comp Neurol 361:249–266.

Gelderman MP, Lefkowitz DL, Lefkowitz SS, Bollen A, Moguilevsky N (1998) Exposure of macrophages to an enzymatically inactive macrophage mannose receptor ligand augments killing of *Candida albicans*. Proc Soc Exp Biol Med 217:81–88.

Giulian D, Baker TJ (1986) Characterization of ameboid microglia isolated from developing mammalian brain. J Neurosci 6:2163–2178.

Giulian D, Robertson C (1990) Inhibition of mononuclear phagocytes reduces ischemic injury in the spinal cord. Ann Neurol 27:33–42.

Giulian D, Vaca K, Corpuz M (1993a) Brain glia release factors with opposing actions upon neuronal survival. J Neurosci 13:29–37.

Giulian D, Corpuz M, Chapman S, Mansouri M, Robertson C (1993b) Reactive mononuclear phagocytes release neurotoxins after ischemic and traumatic injury to the central nervous system. J Neurosci Res 36:681–693.

Giulian D, Li J, Leara B, Keenen C (1994) Phagocytic microglia release cytokines and cytotoxins that regulate the survival of astrocytes and neurons in culture. Neurochem Int 25:227–233.

Grumet M, Flaccus A, Margolis RU (1993) Functional characterization of chondroitin sulfate proteoglycans of brain: interactions with neurons and neural cell adhesion molecules. J Cell Biol 120:815–824.

Guth L (1975) History of central nervous system regeneration research. Exp Neurol 48:3–15.

Guth L, Zhang Z, DiProspero NA, Joubin K, Fitch MT (1994) Spinal cord injury in the rat: treatment with bacterial lipopolysaccharide and indomethacin enhances cellular repair and locomotor function. Exp Neurol 126:76–87.

Hazenbos WL, van den Berg BM, van Furth R (1993) Very late antigen-5 and complement receptor type 3 cooperatively mediate the interaction between Bordetella pertussis and human monocytes. J Immunol 151:6274–6282.

Hazenbos WL, van den Berg BM, Geuijen CW, Mooi FR, van Furth R (1995) Binding of FimD on Bordetella pertussis to very late antigen-5 on monocytes activates complement receptor type 3 via protein tyrosine kinases. J Immunol 155:3972–3978.

Hirschberg DL, Yoles E, Belkin M, Schwartz M (1994) Inflammation after axonal injury has conflicting consequences for recovery of function: rescue of spared axons is impaired but regeneration is supported. J Neuroimmunol 50:9–16.

Ishihara C, Hiratai R, Tsuji M, Yagi K, Nose M, Azuma I (1998) Mannan decelerates the clearance of human red blood cells in SCID mouse. Immunopharmacology 38:223–228.

Issekutz AC, Rowter D, Springer TA (1999) Role of ICAM-1 and ICAM-2 and alternate CD11/CD18 ligands in neutrophil transendothelial migration. J Leukoc Biol 65:117–126.

Jiang C, Ting AT, Seed B (1998) PPAR-gamma agonists inhibit production of monocyte inflammatory cytokines. Nature 391:82–86.

Kao CC, Chang LW, Bloodworth JJ (1977) Axonal regeneration across transected mammalian spinal cords: an electron microscopic study of delayed microsurgical nerve grafting. Exp Neurol 54:591–615.

Kinsella MG, Wight TN (1986) Modulation of sulfated proteoglycan synthesis by bovine aortic endothelial cells during migration. J Cell Biol 102:679–687.

Klegeris A, McGeer PL (1994) Rat brain microglia and peritoneal macrophages show similar responses to respiratory burst stimulants. J Neuroimmunol 53:83–90.

Laywell ED, Dorries U, Bartsch U, Faissner A, Schachner M, Steindler DA (1992) Enhanced expression of the developmentally regulated extracellular matrix molecule tenascin following adult brain injury. Proc Natl Acad Sci USA 89:2634–2638.

Lazarov-Spiegler O, Solomon AS, Zeev-Brann AB, Hirschberg DL, Lavie V, Schwartz M (1996) Transplantation of activated macrophages overcomes central nervous system regrowth failure. FASEB J 10:1296–1302.

Levine JM (1994) Increased expression of the NG2 chondroitin-sulfate proteoglycan after brain injury. J Neurosci 14:4716–4730.

Liu XZ, Xu XM, Hu R, Du C, Zhang SX, McDonald JW, Dong HX, Wu YJ, Fan GS, Jacquin MF, Hsu CY, Choi DW (1997) Neuronal and glial apoptosis after traumatic spinal cord injury. J Neurosci 17:5395–5406.

Lombard Y, Giaimis J, Makaya Kumba M, Fonteneau P, Poindron P (1994) A new method for studying the binding and ingestion of zymosan particles by macrophages. J Immunol Methods 174:155–165.

MacLaren RE (1996) Development and role of retinal glia in regeneration of ganglion cells following retinal injury. Br J Ophthalmol 80:458–464.

Marodi L, Schreiber S, Anderson DC, MacDermott RP, Korchak HM, Johnston Jr RB (1993) Enhancement of macrophage candidacidal activity by interferon-gamma. Increased phagocytosis, killing, and calcium signal mediated by a decreased number of mannose receptors. J Clin Invest 91:2596–2601.

McCarthy KD, De Vellis J (1980) Preparation of separate astroglial and oligodendroglial cell cultures from rat cerebral tissue. J Cell Biol 85:890–902.

McKay PF, Imami N, Johns M, Taylor Fishwick DA, Sedibane LM, Totty NF, Hsuan JJ, Palmer DB, George AJ, Foxwell BM, Ritter MA (1998) The gp200-MR6 molecule which is functionally associated with the IL-4 receptor modulates B cell phenotype and is a novel member of the human macrophage mannose receptor family. Eur J Immunol 28:4071–4083.

McKeon RJ, Schreiber RC, Rudge JS, Silver J (1991) Reduction of neurite outgrowth in a model of glial scarring following CNS injury is correlated with the expression of inhibitory molecules on reactive astrocytes. J Neurosci 11:3398–3411.

Michalek M, Melican D, Brunke Reese D, Langevin M, Lemerise K, Galbraith W, Patchen M, Mackin W (1998) Activation of rat macrophages by Betafectin PGG-glucan requires cross-linking of membrane receptors distinct from complement receptor three (CR3). J Leukoc Biol 64:337–344.

Montero-Menei CN, Sindji L, Pouplard Barthelaix A, Jehan F, Denechaud L, Darcy F (1994) Lipopolysaccharide intracerebral administration induces minimal inflammatory reaction in rat brain. Brain Res 653:101–111.

Muller E, Schroder C, Schauer R, Sharon N (1983) Binding and phagocytosis of sialidase-treated rat erythrocytes by a mechanism independent of opsonins. Hoppe Seylers Z Physiol Chem 364:1419–1429.

Murai M, Aramaki Y, Tsuchiya S (1996) Alpha 2-macroglobulin stimulation of protein tyrosine phosphorylation in macrophages via the mannose receptor for Fc gamma receptor-mediated phagocytosis activation. Immunology 89:436–441.

Noble LJ, Wrathall JR (1985) Spinal cord contusion in the rat: morpho-

metric analyses of alterations in the spinal cord. Exp Neurol 88:135–149.
Popovich PG, Reinhard JF, Flanagan EM, Stokes BT (1994) Elevation of the neurotoxin quinolinic acid occurs following spinal cord trauma. Brain Res 633:348–352.
Prewitt CM, Niesman IR, Kane CJ, Houle JD (1997) Activated macrophage/microglial cells can promote the regeneration of sensory axons into the injured spinal cord. Exp Neurol 148:433–443.
Rabb H, Michishita M, Sharma CP, Brown D, Arnaout MA (1993) Cytoplasmic tails of human complement receptor type 3 (CR3, CD11b/CD18) regulate ligand avidity and the internalization of occupied receptors. J Immunol 151:990–1002.
Rabchevsky AG, Streit WJ (1997) Grafting of cultured microglial cells into the lesioned spinal cord of adult rats enhances neurite outgrowth. J Neurosci Res 47:34–48.
Ramon y Cajal S (1928) Degeneration and regeneration of the nervous system. London: Oxford UP.
Reier PJ, Stensaas LJ, Guth L (1983) The astrocytic scar as an impediment to regeneration in the central nervous system. In: Spinal cord reconstruction (Kao CC, Bunge RP, Reier PJ, eds), pp 163–195. New York: Raven.
Ricote M, Li AC, Willson TM, Kelly CJ, Glass CK (1998) The peroxisome proliferator-activated receptor-gamma is a negative regulator of macrophage activation. Nature 391:79–82.
Ross GD, Vetvicka V (1993) CR3 (CD11b, CD18): a phagocyte and NK cell membrane receptor with multiple ligand specificities and functions. Clin Exp Immunol 92:181–184.
Ross GD, Cain JA, Lachmann PJ (1985) Membrane complement receptor type three (CR3) has lectin-like properties analogous to bovine conglutinin as functions as a receptor for zymosan and rabbit erythrocytes as well as a receptor for iC3b. J Immunol 134:3307–3315.
Schnitzler N, Haase G, Podbielski A, Lutticken R, Schweizer KG (1999) A co-stimulatory signal through ICAM-beta2 integrin-binding potentiates neutrophil phagocytosis. Nat Med 5:231–235.
Snow DM, Lemmon V, Carrino DA, Caplan AI, Silver J (1990) Sulfated proteoglycans in astroglial barriers inhibit neurite outgrowth in vitro. Exp Neurol 109:111–130.
Stewart J, Weir DM (1989) Carbohydrates as recognition molecules in macrophage activities. J Clin Lab Immunol 28:103–108.
Streit WJ, Semple-Rowland SL, Hurley SD, Miller RC, Popovich PG, Stokes BT (1998) Cytokine mRNA profiles in contused spinal cord and axotomized facial nucleus suggest a beneficial role for inflammation and gliosis. Exp Neurol 152:74–87.
Szczepanik AM, Fishkin RJ, Rush DK, Wilmot CA (1996) Effects of chronic intrahippocampal infusion of lipopolysaccharide in the rat. Neuroscience 70:57–65.
Taylor ME (1993) Recognition of complex carbohydrates by the macrophage mannose receptor. Biochem Soc Trans 21:468–473.
Thomas LB, Gates MA, Steindler DA (1996) Young neurons from the adult subependymal zone proliferate and migrate along an astrocyte, extracellular matrix-rich pathway. Glia 17:1–14.
Thornton BP, Vetvicka V, Pitman M, Goldman RC, Ross GD (1996) Analysis of the sugar specificity and molecular location of the beta-glucan-binding lectin site of complement receptor type 3 (CD11b/CD18). J Immunol 156:1235–1246.
Wallace MC, Tator CH, Lewis AJ (1987) Chronic regenerative changes in the spinal cord after cord compression injury in rats. Surg Neurol 27:209–219.
Weintraub BC, Goodnow CC (1998) Immune responses: costimulatory receptors have their say. Curr Biol 8:R575–R577.
Weldon DT, Rogers SD, Ghilardi JR, Finke MP, Cleary JP, O'Hare E, Esler WP, Maggio JE, Mantyh PW (1998) Fibrillar beta-amyloid induces microglial phagocytosis, expression of inducible nitric oxide synthase, and loss of a select population of neurons in the rat CNS *in vivo*. J Neurosci 18:2161–2173.
Wight TN, Kinsella MG, Qwarnstrom EE (1992) The role of proteoglycans in cell adhesion, migration and proliferation. Curr Opin Cell Biol 4:793–801.
Wileman TE, Lennartz MR, Stahl PD (1986) Identification of the macrophage mannose receptor as a 175-kDa membrane protein. Proc Natl Acad Sci USA 83:2501–2505.
Williams B, Terry AF, Jones F, McSweeney T (1981) Syringomyelia as a sequel to traumatic paraplegia. Paraplegia 19:67–80.
Windle WF, Clemente CD, Chambers WW (1952) Inhibition of formation of a glial barrier as a means of permitting a peripheral nerve to grow into the brain. J Comp Neurol 96:359–369.
Xia Y, Vetvicka V, Yan J, Hanikyrova M, Mayadas T, Ross GD (1999) The beta-glucan-binding lectin site of mouse CR3 (CD11b/CD18) and its function in generating a primed state of the receptor that mediates cytotoxic activation in response to iC3b-opsonized target cells. J Immunol 162:2281–2290.
Zhang Z, Krebs CJ, Guth L (1997) Experimental analysis of progressive necrosis after spinal cord trauma in the rat: etiological role of the inflammatory response. Exp Neurol 143:141–152.